White Rose Research Online

eprints@whiterose.ac.uk
https://eprints.whiterose.ac.uk
Universities of Leeds, Sheffield and York

Deposited via The University of Sheffield.

White Rose Research Online URL for this paper:
https://eprints.whiterose.ac.uk/id/eprint/181932/

Version: Accepted Version

Article:
Chang, M.-Y., Tsai, T.-I., Chou, L.-F. et al. (2022) Metformin induces lactate accumulation and accelerates renal cyst progression in Pkd1-deficient mice. Human Molecular Genetics, 31 (10). pp. 1560-1573. ISSN: 0964-6906

https://doi.org/10.1093/hmg/ddab340

This is a pre-copyedited, author-produced version of an article accepted for publication in Human Molecular Genetics following peer review. The version of record: Ming-Yang Chang, Chung-Ying Tsai, Li-Fang Chou, Shen-Hsing Hsu, Huang-Yu Yang, Cheng-Chieh Hung, Ya-Chung Tian, Albert C M Ong, Chih-Wei Yang, Metformin induces lactate accumulation and accelerates renal cyst progression in Pkd1-deficient mice, Human Molecular Genetics, Volume 31, Issue 10, 15 May 2022, Pages 1560–1573, is available online at: https://doi.org/10.1093/hmg/ddab340

Reuse
Items deposited in White Rose Research Online are protected by copyright, with all rights reserved unless indicated otherwise. They may be downloaded and/or printed for private study, or other acts as permitted by national copyright laws. The publisher or other rights holders may allow further reproduction and re-use of the full text version. This is indicated by the licence information on the White Rose Research Online record for the item.

Takedown
If you consider content in White Rose Research Online to be in breach of UK law, please notify us by emailing eprints@whiterose.ac.uk including the URL of the record and the reason for the withdrawal request.

UNIVERSITY OF LEEDS
University of Sheffield
UNIVERSITY of York

Metformin induces lactate accumulation and accelerates renal cyst progression in *Pkd1*-deficient mice

Ming-Yang Chang[1*], Tsung-Inn Tsai[1], Li-Fang Chou[1], Shen-Hsing Hsu[1], Huang-Yu Yang[1], Cheng-Chieh Hung[1], Ya-Chung Tian[1], Albert CM Ong[2], Chih-Wei Yang[1]

[1]Kidney Research Center, Chang Gung Memorial Hospital, Chang Gung University College of Medicine, Taoyuan, Taiwan

[2]Academic Nephrology Unit, Department of Infection, Immunity and Cardiovascular Disease, University of Sheffield, Sheffield, UK

Address correspondence to:

Dr. Ming-Yang Chang[*], Kidney Research Center and Department of Nephrology, Chang Gung Memorial Hospital, 5 Fu-Shing St., Kueishan, Taoyuan, Taiwan.

Phone:+886-3-3281200 EXT.8181 ; Fax: +886-3-3282173 ; E-mail: mingyc@adm.cgmh.org.tw

Abstract

Metabolic reprogramming is a potential treatment strategy for autosomal dominant polycystic kidney disease (ADPKD). Metformin has been shown to inhibit the early stages of cyst formation in animal models. However, metformin can lead to lactic acidosis in diabetic patients with advanced chronic kidney disease, and its efficacy in ADPKD is still not fully understood. Here we investigated the effect of metformin in an established hypomorphic mouse model of PKD that presents stable and heritable knockdown of *Pkd1*. The *Pkd1* miRNA transgenic mice of both genders were randomized to receive metformin or saline injections. Metformin was administrated through daily intraperitoneal injection from postnatal day 35 for 4 weeks. Unexpectedly, metformin treatment at a concentration of 150 mg/kg increased disease severity including kidney-to-body weight ratio, cystic index, and plasma BUN levels, and was associated with increased renal tubular cell proliferation and plasma lactate levels. Functional enrichment analysis for cDNA microarrays from kidney samples revealed significant enrichment of several pro-proliferative pathways including β-catenin, hypoxia-inducible factor-1α, protein kinase Cα, and Notch signaling pathways in the metformin-treated mutant mice. The plasma metformin concentrations were still within the recommended therapeutic range for type 2 diabetic patients. Short-term metformin treatment in a second *Pkd1* hypomorphic model ($Pkd1^{RC/RC}$) was however neutral. These results demonstrate that metformin may exacerbate late-stage cyst growth associated with the activation of lactate-related signaling pathways in *Pkd1*-deficiency. Our findings indicate that using metformin in the later stage of ADPKD might accelerate disease progression and call for the cautious use of metformin in these patients.

Introduction

Autosomal dominant polycystic kidney disease (ADPKD) is a common genetic kidney disease that accounts for 5 to 10 % of patients with end-stage kidney disease (1). The disease is caused by mutations in *PKD1, PKD2,* and other genes such as *DNAJB11* and *GANAB* (2). The pathogenesis of cyst growth in ADPKD is complex and involves fluid secretion, cell proliferation, cilia dysfunction, defective extracellular matrix, and enhanced glycolysis (3). Current disease-specific treatments for ADPKD are limited. Tolvaptan, a vasopressin V2 receptor antagonist, is the first approved drug for ADPKD, but its use is associated with significant aquaretic side effects and rare cases of liver toxicity (4). There is still an urgent need to test alternative treatments that are more effective, safer and better tolerated.

Metabolic reprogramming is a central feature of cystic epithelial cells characterized by the enhanced conversion of glucose to lactate and reduced oxidative phosphorylation in mitochondria, resembling the Warburg effect originally found in cancer cells (5). *PKD1*-deficient cells produce more lactate due to enhanced aerobic glycolysis (6). This is associated with increased cell proliferation, reduced autophagy, and activation of complex signaling pathways that promotes cystogenesis. Novel treatment strategies to retard cyst progression by metabolic reprogramming include 2-deoxy-d-glucose (7), caloric restriction and the induction of ketosis to inhibit glycolysis (8-10).

Metformin is a widely prescribed oral anti-diabetic agent that has been proposed to treat ADPKD due to its ability to enhance the action of AMP-activated protein kinase (AMPK) in suppressing mammalian target of rapamycin (mTOR) and the cystic fibrosis transmembrane conductance regulator (CFTR) in animal models of early PKD (11-13). Short-term (~2-10 days) metformin treatment retarded cyst expansion in neonatal *Pkd1*-knockout mice and *pkd2* zebrafish morphants (11, 12),

whereas chronic treatment (~10 weeks) did not protect against cyst growth in adult-onset conditional *Pkd1*-knockout mice (14). However, metformin suppresses hepatic gluconeogenesis by inhibiting mitochondrial glycerophosphate dehydrogenase thus reducing the conversion of lactate and glycerol to glucose in the liver independently of AMPK (15-17). Metformin can cause an infrequent but potentially life-threatening complication of lactic acidosis and is contraindicated in advanced chronic kidney disease (CKD) (18). Whether metformin can modify disease progression in ADPKD remains unclear.

Here we investigated the effect of chronic metformin administration on cyst growth and disease progression in a hypomorphic *Pkd1* mouse model. Surprisingly, metformin led to a more severe cystic phenotype associated with increased lactate accumulation and the activation of pro-proliferative pathways. Our findings reveal a potential adverse effect of metformin in the later stages of ADPKD and call for the cautious use of metformin in these patients.

Results

Effects of metformin on kidney weight and cyst volume

We determined the effects of metformin on cyst growth and renal function in *Pkd1* miR Tg mice which represents a chronic progressive mouse model of ADPKD. Rapid cyst growth occurs from approximately postnatal day (P) 14 to P60 in this model (predominantly from distal nephron segments) and kidney function declines slowly from P30 as has been described previously (19, 20). Therefore, the treatment period (P35 to P62) in our study would be equivalent to CKD stage 3 in humans. Female and male *Pkd1*-deficient mice and wild-type littermates were randomized to receive intraperitoneal (i.p.) metformin (150 mg/kg/day; n=15 for *Pkd1;* n=7 for wild-type) or vehicle (0.9% saline; n=14 for *Pkd1* and n=8 for wild-type) for 28 days (Figure 1a, Supplementary Table S2). To assess the potential dose-dependent effects, additional groups of *Pkd1*-deficient mice were randomized to receive low-dose metformin (75 mg/kg/day; n=8) or vehicle (0.9% saline, n=8) injections. Surprisingly, we found that the average kidney-to-body weight ratio was significantly increased by 53% in the metformin-treated group (150 mg/kg/day) compared with the vehicle-treated group (3.63±0.20 vs. 2.37±0.08, $P<0.001$; Figure 1b and c). The kidney-to-body weight was also increased by 16% in the low-dose (75 mg/kg/day) group but this is not statistically significant (2.74±0.25 vs. 2.37±0.08, $P>0.05$). *Pkd1*-deficient mice treated with metformin (150 mg/kg/day) also showed a 24 % increase of cystic index compared to those treated with vehicle (38.2 % vs 30.9 %, $P<0.001$; Figure 1d), confirming that metformin treatment resulted in a more severe cystic phenotype. No significant gender effects of metformin treatment were found (Supplementary Figure S1). The expression of transgenic *Pkd1-miRNAs* was not significantly different between groups (Supplementary Figure S2).

Effects of metformin on renal function

Consistent with a more severe cystic phenotype in metformin-treated Tg mice, renal function was significantly impaired with metformin treatment. Blood urea nitrogen (BUN) levels were significantly increased in the metformin-treated *Pkd1*-deficient mice (150 mg/kg/day) compared to vehicle-treated *Pkd1* control (47.7±3.1 vs. 38.6±2.5 mg/dl, $P<0.01$; Figure 1e). Plasma Cystatin-C levels were also significantly increased in the metformin group (150 mg/kg/day) compared to the vehicle group (692.7±24.0 vs. 599.6±21.1, $P<0.05$, Supplementary Table S2). Non-fasting glucose levels were not significantly different between groups (Supplementary Table S2). There was no increased mortality in all groups of mice, excluding significant toxicity from metformin treatment. These results demonstrate that chronic treatment with metformin led to a worsening of renal function in *Pkd1*-deficient mice without affecting survival.

Metformin treatment in *Pkd1*$^{RC/RC}$ mice

We tested the effect of metformin in a second hypomorphic *Pkd1* model, *Pkd1*$^{RC/RC}$ mice, which develops more slowly progressive disease (21). *Pkd1*$^{RC/RC}$ mice were also treated with i.p metformin (150 mg/kg/day) from P35 to P64 and compared to vehicle-treated mutant mice (n=6 males per group). In this model, metformin had no significant effect on renal function or other disease markers such as kidney-to-body weight ratio, cystic index, plasma BUN, cystatin-C, and lactate levels (Supplementary Figure S3). Cystic disease was milder and more variable in this model compared to *Pkd1* miR Tg mice so a significant effect might have been missed due to the small sample size and relatively short treatment duration (30d) in this more chronic model. Alternatively, a difference in the tempo of disease initiation might account for the differential response to metformin in both models.

Effects of metformin on cyst growth and cell proliferation

To determine if metformin treatment is associated with enhanced tubular cell proliferation, we performed immunohistochemistry staining for the cell proliferation marker proliferating cell nuclear antigen (PCNA) in *Pkd1* miR Tg mice. A significant increase in the proliferative index was found in the cystic kidneys of *Pkd1*-deficient mice compared with wild-type mice, and this was further enhanced after metformin treatment (150 mg/kg/day) (Figure 2). These data suggest that chronic administration of metformin in later-stage PKD may enhance cell proliferation and promote cyst growth.

Effect of metformin on renal fibrosis and macrophage infiltration

To investigate if changes in extracellular matrix could be a primary target of metformin, we examined the effects of metformin (150 mg/kg/day) on renal fibrosis and macrophage infiltration. Despite a more severe cystic phenotype, the degree of renal fibrosis was unchanged by metformin (Figure 3a and b). Renal mRNA expression of *Col1a2* and *Fn1* was not different after metformin treatment (Figure 3c and d) but there was a small reduction in *Tgfb1* expression ($P<0.05$; Figure 3e). No significant differences in the percentage of F4/80-positive macrophages or in the mRNA of inflammatory-related genes (*Il1b*, *Tnf, Mcp1,* and *Il34)* were detected (Figure 4) apart from a small reduction in *Il6* mRNA expression in the metformin group ($P<0.001$). These results indicate that the major effects of metformin on cyst growth are unlikely to be mediated through macrophage infiltration or renal fibrosis.

Metformin induces lactate accumulation

We next determined plasma concentrations of lactate in these mice (Figure 5a).

Plasma lactate concentrations were 35% higher in metformin-treated *Pkd1*-deficient mice (150 mg/kg/day) compared to their vehicle-treated *Pkd1* littermates (10.5±0.6 mM vs 7.1±0.4 mM, $P<0.001$). In wild-type mice, plasma lactate concentrations were also significantly increased in the metformin group compared with untreated controls (12.5±1.3 mM vs 6.2±0.5 mM, $P<0.001$). There were no significant differences in plasma lactate levels between wild-type and *Pkd1* miR Tg mice. A lower dose of metformin (75 mg/kg/day) did not significantly alter lactate levels. Of relevance, plasma lactate levels were significantly correlated to kidney/body weights, cystic indices, and BUN levels in *Pkd1*-deficient mice (Figure 5b-d).

Activation of pro-proliferative pathways with metformin treatment

To determine the differentially expressed genes affected by metformin treatment, We performed a microarray analysis using cDNA from the kidney tissues of vehicle- and metformin-treated *Pkd1*-deficient mice (n=3 each). Principal Component Analysis (PCA) of microarray data revealed a different gene expression profile between the two groups (Figure 6a). The top 100 differentiated expressed genes (fold change > 2, $P<0.05$) are presented on a heat map (Supplementary Figure S4). We further analyzed the transcriptome using GSEA by comparing our microarray data with gene sets in the database correlated to known signaling pathways (22). Consistent with the phenotypic changes of renal cysts, we found that four pro-proliferative pathways, including β-catenin, protein kinase C alpha (PKCα), hypoxia-inducible factor-1α (HIF-1α) and Notch pathways were significantly enriched ($P<0.01$), while the autophagy pathway was significantly reduced ($P<0.01$) in the metformin group (Figure 6 b-f). We validated the canonical Wnt (β-catenin) pathway and AMPK in the kidney samples by Western blot analysis (Figure 7a and b). Indeed, active β-catenin expression was significantly elevated in the metformin group, supporting the activation of this

pathway. Surprisingly, we found a significant reduction in the level of phosphorylated AMPK in the kidneys of metformin-treated mutant mice. This was unexpected as metformin is a known AMPK activator (11). However, the reduced activation of AMPK is consistent with the defective cellular metabolism associated with increased cyst severity. We did not observe significant changes in the phosphorylation of mTOR (Supplementary Figure S5) or extracellular signal-regulated kinases (ERK) (Supplementary Figure S6) following metformin treatment in *Pkd1*-deficient mice, suggesting that metformin could act via an AMPK/mTOR independent pathway.

Suppression of glucose metabolism with metformin treatment

Previous studies have proposed that metformin causes lactate accumulation by inhibiting pyruvate carboxylase (*Pcx*) and pyruvate dehydrogenase (*Pdhx*)(15). Indeed, the mRNA expression of both *Pcx* and *Pdhx* were significantly reduced in *Pkd1*-deficient cystic kidneys following metformin treatment (Figure 8a). We also found metformin significantly suppressed the expression of *Hk1* and *Hk2,* two key regulators in the glycolytic pathway, and *Monocarboxylate transporter 4 (Slc16a3)* which exports intracellular lactate (Figure 8a). Expression of the von Hippel-Lindau (*Vhl*) tumor suppressor gene, a negative regulator for HIF-1α, was also significantly reduced in the metformin-treated mutant mice (Figure 8a). In line with previous studies, a significant reduction in autophagy-related genes including *Atg5, Atg12, Ulk1, Becn1,* and *Vps34* was found in *Pkd1*-deficient mice compared to controls by qRT-PCR(23), but metformin treatment did not rescue the deficiency (Figure 8b).

Plasma concentrations of metformin

To confirm the relevance of these findings to therapeutic metformin doses used clinically, we measured the blood concentrations of metformin by liquid

chromatography-mass spectrometry (LC-MS). The metformin concentrations in *Pkd1*-deficient mice treated with 150 mg/kg/day of metformin were significantly higher (13.7±1.6 μM) than those in wild-type mice treated with the same dose (8.1±1.5 μM, $P<0.05$) or *Pkd1*-deficient mice treated with 75 mg/kg/day of metformin (5.2±0.6 μM, $P<0.01$) (Figure 9a). Further analysis revealed significant correlations between blood metformin concentrations and BUN ($P<0.001$) or cystatin C levels ($P<0.0001$) (Figure 9b and c) consistent with its dependence on renal excretion. Metformin concentrations also showed a significant positive correlation to kidney/body weights ($P<0.01$), cystic indices ($P<0.05$), and plasma lactate levels ($P<0.01$) in *Pkd1*-deficient mice (Figure 9d-f), suggesting a dose-dependent effect. These concentrations are within the recommended therapeutic range for treating type 2 diabetes patients (24), suggesting that our data could be broadly applicable to ADPKD.

Discussion

Contrary to previous studies in animal models of rapid-onset ADPKD (11, 12), we did not find a beneficial effect of metformin on cyst growth in two chronic progressive *Pkd1*-deficient mouse models. We found that metformin conferred no benefit in preventing cyst progression and could even accelerate cyst growth in the later stages of ADPKD. Our study provides the first *in vivo* evidence that metformin treatment may lead to increased lactate accumulation and accelerate the progression of polycystic kidney disease.

Several explanations may account for the discrepancy between our results and previous studies. Firstly, we administrated metformin from P35 in *Pkd1*-deficient mice after cyst development for four weeks, a different strategy from the short-term treatment (P7 to P17) in neonatal *Pkd1*-knockout mice started before cyst initiation (11): this could suggest a better response to metformin in the early stages of cyst formation compared to the setting of established cysts and renal function impairment. Secondly, the metformin concentrations achieved in our study were much lower than the concentrations (in the mM range) found to inhibit cyst growth in cell-based and zebrafish models (11, 12). However, it would be unrealistic to achieve such high clinical concentrations of metformin without significant side effects. The dose of metformin (150 mg/kg/day) used in our study is equivalent to approximately 12.5 mg/kg/day in humans if corrected by body surface area (25). Of note, we have measured the actual concentrations of metformin in our study and the results (13.7±1.6 μM) were consistent with the known therapeutic levels in humans for type 2 diabetes (6-30 μM) (24, 26). Since the plasma metformin levels of the current study are still within the therapeutic range, the accelerated cystic phenotype observed is likely to be clinically relevant to ADPKD.

Our results are partially consistent with the study of Leonhard et al. reporting

that administration of metformin in drinking water did not affect cyst formation in an adult-onset conditional *Pkd1*-knockout mouse model (14). The discrepancy might be attributed to different mouse models used (*Pkd1* knockout vs. knockdown) or different routes of metformin administration. Compared to continuous oral administration of metformin, the intermittent pulse i.p. injection in our study might achieve a higher peak plasma concentration of metformin which could increase the chance of lactate accumulation (15). Nevertheless, these findings are in agreement with the observation in mice that metformin (0.1% w/w in diet) extended their lifespan but a higher dose (1% w/w) induced enlarged 'lumpy' kidneys with associated kidney failure and a reduced lifespan (27).

The elevation of lactate levels in metformin-treated *Pkd1* mutant mice is associated with a more severe cystic phenotype in our study, indicating a potential role of lactate on the progression of ADPKD. Lactate accumulation has also been shown to promote cyst-lining epithelial cell proliferation in a rapid-onset *Pkd1* mouse model (28). Although metformin inhibits hepatic gluconeogenesis, excessive lactate accumulation in the *Pkd1*-deficient kidney cells can be recycled through the "lactate shuttle" to pyruvate, leading to ATP generation through oxidative phosphorylation which could promote cell proliferation (29, 30). Lactate accumulation in the kidneys could be a high-energy nutrient for cell proliferation and cyst growth (31). Excessive lactate production may also suppress AMPK phosphorylation due to an increased ATP/AMP ratio (32-34). A similar concept has been found in the cancer microenvironment where lactate acts as an important oncometabolite that regulates both intracellular and extracellular signaling pathways associated with cancer progression (35-37). This 'pseudohypoxia' state could also lead to activation of the HIF/Wnt/β-catenin pathway and downstream cystogenic pathways (32, 38). Our results are consistent with the important role of β-catenin activation in the

pathogenesis of ADPKD (39, 40). The reactivation of developmental pathways such as Notch and PKCα pathways following injury and repair can also accelerate the progression of ADPKD (41, 42). Therefore, metformin-induced lactate accumulation could be a "third-hit" to induce proliferation and disease progression in PKD (Figure 10)(43). Further studies such as using lactate dehydrogenase (LDH) inhibitors to reduce lactate accumulation would be helpful to determine the effects and mechanisms of lactate on cystogenesis.

Metformin treatment did not efficiently activate AMPK in our study, which may account for the lack of efficacy in suppressing renal cystogenesis. Intermittent intraperitoneal administration of metformin in our study may not achieve renal concentrations sufficient for sustained AMPK activation (~1 mM *in vitro)*(11). However, as we did achieve therapeutic metformin concentrations and found lactate accumulation at these doses, it is unlikely a higher dose would be beneficial for preventing cyst growth. Nevertheless, the reduced AMPK phosphorylation in metformin-treated *Pkd1*-deficient mice was unexpected. This could relate to a more severe cystic phenotype with metabolic changes secondary to activation of other pro-proliferative pathways induced by metformin (44). Our results support previous reports that metformin can act through an AMPK-independent mechanism and has a pleiotropic effect (13).

A limitation of this study is that we did not start metformin treatment from the neonatal period and therefore cannot exclude the potential therapeutic effects of metformin on early cystogenesis. Our present data suggest that the accelerating effect of metformin in the *Pkd1* miRNA knockdown mouse which develops moderately progressive disease (19) is stronger than that seen in a more chronic *Pkd1* model (*Pkd1* $^{RC/RC}$) for a similar treatment duration. Further study in additional *Pkd1* models (early-onset or late-onset) will be needed to clarify this observation. A recent Phase 2

trial of metformin in ADPKD patients with an eGFR >50 ml/min/1.73m^2 showed no significant adverse effects but with inconclusive efficacy on renal function decline and a trend toward increased total kidney volume (45). It is worth noting that metformin is solely excreted by the kidneys and can cause lactic acidosis in patients with advanced CKD (46). Although our results will need to be confirmed in other PKD models and humans, our present data do raise concerns and questions regarding the use of metformin in ADPKD patients with lower eGFR. As metformin treatment could pose potential risks of adverse effects in late-stage ADPKD (47), monitoring lactate levels might be necessary for ADPKD patients receiving metformin even when the eGFR is >30 (CKD3).

In conclusion, we report that metformin induces lactate accumulation and exacerbates kidney cyst growth in *Pkd1*-deficient mice through the activation of pro-proliferative signaling pathways. Our study demonstrates that metformin might not be beneficial for slowing the progression of ADPKD and could have adverse effects associated with lactate metabolism. These findings indicate that using metformin in the later stage of ADPKD might accelerate disease progression and call for cautious use of metformin and monitoring of blood lactate levels in these patients.

Materials and Methods

Animal Model

Pkd1 miRNA transgenic *(Pkd1* miR Tg) mice were obtained from the National Rodent Model Resource Center (Tainan, Taiwan). The mutant mice express miRNA hairpins specific to *Pkd1* transcript, resulting in stable and heritable *Pkd1* knockdown (~70%) and progressive renal cystogenesis as described in detail previously (19, 20). Wild-type littermate*s* were used as controls. $Pkd1^{RC/RC}$ knockin mice, a slowly progressive PKD model matching the PKD1 p.R3277C (RC) mutation, were a kind gift of Dr. Peter Harris (Mayo Clinic) (21). All the mice were housed in the Chang Gung Memorial Hospital Animal Center (Taoyuan, Taiwan) under climate-controlled conditions with a 12-hour light-dark cycle. The mice were fed standard chow and water *ad lib*. The study was approved by the Animal Care and Use Committee of Chang Gung Memorial Hospital in accordance with the National Institute of Health Guide for the Care and Use of Laboratory Animals.

Experimental Design

Pkd1 miR Tg mice and wild-type littermates of both genders were randomized into experimental and control groups. The experimental groups received metformin (75 or 150 mg/kg body weight in sterile 0.9% saline; Enzo, Farmingdale, NY) administrated by daily i.p. injections from P35 to P62. The control groups were treated with 0.9% saline through daily i.p. injections. The dosage of metformin used achieved plasma concentrations close to the steady-state values reported in patients(16, 48). Non-fasting glucose levels were measured by tail vein sampling using a portable glucometer on P48 and P61

Laboratory parameters

Mice were anesthetized and sacrificed two hours after the final dose of metformin or vehicle on P62. Blood samples were collected through cardiac puncture under anesthesia. Both kidneys were harvested and the weights were measured immediately. BUN levels were measured using a mouse-specific enzyme-linked immunosorbent assay (ELISA) kit (BioAssay, Hayward, CA). Cystatin C was measured using a mouse/rat Cystatin C Quantikine ELISA kit (R&D, Minneapolis, MN)(9). Plasma L-lactate levels were determined using the EnzyChrom L-Lactate Assay Kit (BioAssay).

Histomorphometric analysis

Kidney samples were fixed in 10% neutral-buffered formalin overnight, transferred to 75% ethanol, and embedded in paraffin for sectioning. Transverse kidney sections (4-μm thick) were stained with Hematoxylin & Eosin. The cystic index (percentage) was determined by dividing the area of the cystic lumen by the total kidney area using MetaMorph software (Universal Imaging, West Chester, PA). Masson's trichrome staining was performed to assess the severity of renal fibrosis according to standard protocol. The fibrotic area percentage was calculated in five consecutively selected fields of the renal cortex and medulla at 100× magnification. All analyses were performed on coded slides in a single-blinded manner.

Immunohistochemistry

Paraffin-embedded kidney sections were dewaxed, rehydrated, boiled in citrate buffer (pH 6.0) for heat-induced antigen retrieval, and blocked with Rodent Block M (RBM961H; Biocare, Concord, CA). The sections were stained with a mouse monoclonal anti-PCNA antibody (1:2000, PC10; Cell Signaling, Danvers, MA) for 1 hour at 37°C, followed by incubation with Mouse-on-Mouse horseradish

peroxidase(HRP)-polymer (RMR510H; Biocare, Concord, CA). F4/80 immunostaining was performed using a rat anti-mouse F4/80 antibody (1:100, MCA497R; Serotec, Oxford, UK) overnight at 4°C, followed by a biotin-conjugated goat anti-rat light chain antibody (1:1000, AP202B; Merck Millipore, Darmstadt, Germany) and Streptavidin HRP Label (HP604H; Biocare). The reactions were visualized using 3,3'-diaminobenzidine (DAB) chromogen and counterstained with hematoxylin. The proliferative index was determined by counting the number of PCNA-positive epithelial cells at 200× magnification in consecutively selected fields. The percentage area of F4/80-positive staining was determined in five sequentially fields at 100× magnification.

Quantitative RT-PCR

Total RNA was extracted from snap-frozen kidney tissues using TRIzol reagent (Invitrogen, Carlsbad, CA) according to the manufacturer's protocol. The Transcriptor First-Strand Synthesis Kit (Roche, Indianapolis, IN) was used for the first-strand cDNA synthesis. Quantitative real-time polymerase chain reaction (qRT-PCR) was performed in duplicate using an ABI ViiA7 sequence detection system (Applied Biosystems, Foster City, CA) with TaqMan assays or SYBR Green primers (Supplementary Table S1). The relative mRNA expression levels were calculated using the 2-ddCt method with TATA-binding protein (TBP) as endogenous controls. Transgenic *Pkd1*-miRNAs were measured using TaqMan MicroRNA Reverse Transcription Kit (Applied Biosystems) and qRT-PCR with SYBR Green primers as reported previously(19).

Western blotting

Proteins were isolated from homogenized frozen kidney specimens following

standard procedures. Equal amounts of total protein were separated by sodium dodecyl sulfate-polyacrylamide gel electrophoresis and then transferred onto a polyvinylidene fluoride membrane (Millipore, Bedford, MA). After blocking in 5% fat-free milk, membranes were incubated with primary antibodies including anti-phospho-AMPKα (Thr172), anti-AMPKα, anti-phospho-mTOR (Ser2448), anti-mTOR, anti-active-β-Catenin (Ser33/37/Thr41), anti-phospho-ERK1/2 (Thr202/Tyr204), anti-ERK1/2 (Cell Signaling Technology, Danvers, MA), anti-GAPDH, and anti-β-actin (Abcam, Cambridge, UK) at 4°C overnight. Membranes were further incubated with HRP-conjugated secondary antibodies at room temperature and the signals were detected by enhanced chemiluminescence. Densitometry analysis was performed using ImageJ software (NIH).

Plasma metformin concentration

Plasma metformin levels were determined by LC-MS. Plasma samples (10 μL) were extracted with methanol and centrifuged for 10 minutes at 12000 g. The supernatant was dried with nitrogen and re-dissolved with 100 μL water and analyzed on ultra-high-performance liquid chromatography coupled with Xevo TQ-S MS (Waters, Milford, MA).

Gene expression profiling with microarray

We performed a microarray analysis on the RNA samples from the cystic kidneys of *Pkd1* miR Tg mice treated with vehicle and metformin (n=3 each). the Clariom D Assay (#902513) and GeneChip WT PLUS Reagent Kit (#902280, Thermo Fisher Scientific, Waltham, MA) were used following standard protocol. Data processing was performed using Applied Biosystems Transcriptome Analysis Console (TAC) version 4.0 with Gene Level-SST RMA normalization method. The microarray

data have been deposited in the Gene Expression Omnibus (GEO) database under accession number GSE154590.

Gene Set Enrichment Analysis (GSEA)

Gene set enrichment analysis (GSEA: www.broad.mit.edu/GSEA) was performed to explore the biological pathways involved in metformin-induced cyst growth(49). We used the built-in C2, C5 and C6 curated gene sets from Molecular Signatures Database (MSigDB 6.0: www.broadinstitute.org/gsea/msigdb). The statistical significance of GSEA was analyzed using 1000 permutations. Enrichment was compared between the vehicle-treated *Pkd1* miR Tg mice and those treated with metformin. A positive enrichment score indicates that the specific molecular signature correlated with the phenotype of the vehicle-treated *Pkd1*-deficient mice. The resulted pathways are selected using the normalized enrichment score (NES)>1 and nominal $P<0.05$.

Statistical analysis

Values are expressed as mean±SEM. Between-group comparisons were performed using one-way ANOVA followed by the Newman-Keuls Multiple Comparison Test. Pearson correlation. Differences were considered statistically significant if $P<0.05$. All analyses were performed using GraphPad Prism 5 (GraphPad, La Jolla, CA).

Acknowledgments

We thank Prof. Si-Tse Jiang for providing the *Pkd1 miR* Tg mice (National Laboratory Animal Center, Taiwan), Prof. Mei-Ling Cheng (Chang Gung University, Taiwan) for providing the service of mass spectrometry for metformin concentrations,

and Hui-Wen Chiang, Yi-Ching Ko, Chiung-Tzeng Huang, and Jing-Shiuan Liu for their technical assistance. We also thank the technical assistance of Genomic Medicine Core Laboratory (Chang Gung Memorial Hospital, Linkou).

Conflict of Interest Statement

None declared

Funding

This work was supported by grants from the Chang Gung Memorial Hospital [CMRPG3E2002, 3H0072, 3J1911] and the Ministry of Science and Technology of Taiwan [MOST 104-2314-B-182A-114, 107-2314-B-182A-016].

References

1. Spithoven, E.M., Kramer, A., Meijer, E., Orskov, B., Wanner, C., Abad, J.M., Areste, N., de la Torre, R.A., Caskey, F., Couchoud, C. *et al.* (2014) Renal replacement therapy for autosomal dominant polycystic kidney disease (ADPKD) in Europe: prevalence and survival--an analysis of data from the ERA-EDTA Registry. *Nephrol. Dial. Transplant.*, **29 Suppl 4**, iv15-25.
2. Cornec-Le Gall, E., Audrezet, M.P., Chen, J.M., Hourmant, M., Morin, M.P., Perrichot, R., Charasse, C., Whebe, B., Renaudineau, E., Jousset, P. *et al.* (2013) Type of PKD1 mutation influences renal outcome in ADPKD. *J. Am. Soc. Nephrol.*, **24**, 1006-1013.
3. Chang, M.Y. and Ong, A.C.M. (2018) Targeting new cellular disease pathways in autosomal dominant polycystic kidney disease. *Nephrol. Dial. Transplant.*, **33**, 1310-1316.
4. Torres, V.E., Chapman, A.B., Devuyst, O., Gansevoort, R.T., Perrone, R.D., Koch, G., Ouyang, J., McQuade, R.D., Blais, J.D., Czerwiec, F.S. *et al.* (2017) Tolvaptan in Later-Stage Autosomal Dominant Polycystic Kidney Disease. *N. Engl. J. Med.*, **377**, 1930-1942.
5. Nowak, K.L. and Hopp, K. (2020) Metabolic Reprogramming in Autosomal Dominant Polycystic Kidney Disease: Evidence and Therapeutic Potential. *Clin. J. Am. Soc. Nephrol.*, **15**, 577-584.
6. Rowe, I., Chiaravalli, M., Mannella, V., Ulisse, V., Quilici, G., Pema, M., Song, X.W., Xu, H., Mari, S., Qian, F. *et al.* (2013) Defective glucose metabolism in polycystic kidney disease identifies a new therapeutic strategy. *Nat. Med.*, **19**, 488-493.
7. Chiaravalli, M., Rowe, I., Mannella, V., Quilici, G., Canu, T., Bianchi, V., Gurgone, A., Antunes, S., D'Adamo, P., Esposito, A. *et al.* (2016) 2-Deoxy-d-Glucose Ameliorates PKD Progression. *J. Am. Soc. Nephrol.*, **27**, 1958-1969.
8. Riwanto, M., Kapoor, S., Rodriguez, D., Edenhofer, I., Segerer, S. and Wuthrich, R.P. (2016) Inhibition of Aerobic Glycolysis Attenuates Disease Progression in Polycystic Kidney Disease. *PLoS One*, **11**, e0146654.
9. Warner, G., Hein, K.Z., Nin, V., Edwards, M., Chini, C.C., Hopp, K., Harris, P.C., Torres, V.E. and Chini, E.N. (2016) Food Restriction Ameliorates the Development of Polycystic Kidney Disease. *J. Am. Soc. Nephrol.*, **27**, 1437-1447.
10. Torres, J.A., Kruger, S.L., Broderick, C., Amarlkhagva, T., Agrawal, S., Dodam, J.R., Mrug, M., Lyons, L.A. and Weimbs, T. (2019) Ketosis Ameliorates Renal Cyst Growth in Polycystic Kidney Disease. *Cell Metab.*, **30**, 1007-1023 e1005.
11. Takiar, V., Nishio, S., Seo-Mayer, P., King, J.D., Jr., Li, H., Zhang, L., Karihaloo, A., Hallows, K.R., Somlo, S. and Caplan, M.J. (2011) Activating AMP-activated protein kinase (AMPK) slows renal cystogenesis. *Proc. Natl Acad. Sci. U S A*, **108**, 2462-2467.

12. Chang, M.Y., Ma, T.L., Hung, C.C., Tian, Y.C., Chen, Y.C., Yang, C.W. and Cheng, Y.C. (2017) Metformin Inhibits Cyst Formation in a Zebrafish Model of Polycystin-2 Deficiency. *Sci. Rep.*, **7**, 7161.
13. Agius, L., Ford, B.E. and Chachra, S.S. (2020) The Metformin Mechanism on Gluconeogenesis and AMPK Activation: The Metabolite Perspective. *Int. J. Mol. Sci.*, **21**.
14. Leonhard, W.N., Song, X., Kanhai, A.A., Iliuta, I.A., Bozovic, A., Steinberg, G.R., Peters, D.J.M. and Pei, Y. (2019) Salsalate, but not metformin or canagliflozin, slows kidney cyst growth in an adult-onset mouse model of polycystic kidney disease. *EBioMedicine*, **47**, 436-445.
15. Oyaizu-Toramaru, T., Suhara, T., Hayakawa, N., Nakamura, T., Kubo, A., Minamishima, S., Yamaguchi, K., Hishiki, T., Morisaki, H., Suematsu, M. *et al.* (2017) Targeting Oxygen-Sensing Prolyl Hydroxylase for Metformin-Associated Lactic Acidosis Treatment. *Mol. Cell. Biol.*, **37**.
16. Madiraju, A.K., Erion, D.M., Rahimi, Y., Zhang, X.M., Braddock, D.T., Albright, R.A., Prigaro, B.J., Wood, J.L., Bhanot, S., MacDonald, M.J. *et al.* (2014) Metformin suppresses gluconeogenesis by inhibiting mitochondrial glycerophosphate dehydrogenase. *Nature*, **510**, 542-546.
17. Madiraju, A.K., Qiu, Y., Perry, R.J., Rahimi, Y., Zhang, X.M., Zhang, D., Camporez, J.G., Cline, G.W., Butrico, G.M., Kemp, B.E. *et al.* (2018) Metformin inhibits gluconeogenesis via a redox-dependent mechanism in vivo. *Nat. Med.*, **24**, 1384-1394.
18. Lazarus, B., Wu, A., Shin, J.I., Sang, Y., Alexander, G.C., Secora, A., Inker, L.A., Coresh, J., Chang, A.R. and Grams, M.E. (2018) Association of Metformin Use With Risk of Lactic Acidosis Across the Range of Kidney Function: A Community-Based Cohort Study. *JAMA Intern. Med.*, **178**, 903-910.
19. Wang, E., Hsieh-Li, H.M., Chiou, Y.Y., Chien, Y.L., Ho, H.H., Chin, H.J., Wang, C.K., Liang, S.C. and Jiang, S.T. (2010) Progressive renal distortion by multiple cysts in transgenic mice expressing artificial microRNAs against Pkd1. *J. Pathol.*, **222**, 238-248.
20. Chou, L.F., Cheng, Y.L., Hsieh, C.Y., Lin, C.Y., Yang, H.Y., Chen, Y.C., Hung, C.C., Tian, Y.C., Yang, C.W. and Chang, M.Y. (2018) Effect of Trehalose Supplementation on Autophagy and Cystogenesis in a Mouse Model of Polycystic Kidney Disease. *Nutrients*, **11**.
21. Hopp, K., Ward, C.J., Hommerding, C.J., Nasr, S.H., Tuan, H.F., Gainullin, V.G., Rossetti, S., Torres, V.E. and Harris, P.C. (2012) Functional polycystin-1 dosage governs autosomal dominant polycystic kidney disease severity. *J. Clin. Invest.*, **122**, 4257-4273.
22. Subramanian, A., Tamayo, P., Mootha, V.K., Mukherjee, S., Ebert, B.L., Gillette,

M.A., Paulovich, A., Pomeroy, S.L., Golub, T.R., Lander, E.S. *et al.* (2005) Gene set enrichment analysis: a knowledge-based approach for interpreting genome-wide expression profiles. *Proc. Natl Acad. Sci. U S A*, **102**, 15545-15550.
23. Zhu, P., Sieben, C.J., Xu, X., Harris, P.C. and Lin, X. (2017) Autophagy activators suppress cystogenesis in an autosomal dominant polycystic kidney disease model. *Hum. Mol. Genet.*, **26**, 158-172.
24. Biondani, G. and Peyron, J.F. (2018) Metformin, an Anti-diabetic Drug to Target Leukemia. *Front. Endocrinol. (Lausanne)*, **9**, 446.
25. Reagan-Shaw, S., Nihal, M. and Ahmad, N. (2008) Dose translation from animal to human studies revisited. *FASEB J.*, **22**, 659-661.
26. He, L. and Wondisford, F.E. (2015) Metformin action: concentrations matter. *Cell Metab.*, **21**, 159-162.
27. Martin-Montalvo, A., Mercken, E.M., Mitchell, S.J., Palacios, H.H., Mote, P.L., Scheibye-Knudsen, M., Gomes, A.P., Ward, T.M., Minor, R.K., Blouin, M.J. *et al.* (2013) Metformin improves healthspan and lifespan in mice. *Nat. Commun.*, **4**, 2192.
28. Yang, Y., Chen, M., Zhou, J., Lv, J., Song, S., Fu, L., Chen, J., Yang, M. and Mei, C. (2018) Interactions between Macrophages and Cyst-Lining Epithelial Cells Promote Kidney Cyst Growth in Pkd1-Deficient Mice. *J. Am. Soc. Nephrol.*, **29**, 2310-2325.
29. Wilde, L., Roche, M., Domingo-Vidal, M., Tanson, K., Philp, N., Curry, J. and Martinez-Outschoorn, U. (2017) Metabolic coupling and the Reverse Warburg Effect in cancer: Implications for novel biomarker and anticancer agent development. *Semin. Oncol.*, **44**, 198-203.
30. Takiyama, Y. and Haneda, M. (2014) Hypoxia in diabetic kidneys. *Biomed. Res. Int.*, **2014**, 837421.
31. Fu, Y., Liu, S., Yin, S., Niu, W., Xiong, W., Tan, M., Li, G. and Zhou, M. (2017) The reverse Warburg effect is likely to be an Achilles' heel of cancer that can be exploited for cancer therapy. *Oncotarget*, **8**, 57813-57825.
32. Zhang, G., Darshi, M. and Sharma, K. (2018) The Warburg Effect in Diabetic Kidney Disease. *Semin. Nephrol.*, **38**, 111-120.
33. Harun-Or-Rashid, M. and Inman, D.M. (2018) Reduced AMPK activation and increased HCAR activation drive anti-inflammatory response and neuroprotection in glaucoma. *J. Neuroinflammation*, **15**, 313.
34. Carneiro, L., Asrih, M., Repond, C., Sempoux, C., Stehle, J.C., Leloup, C., Jornayvaz, F.R. and Pellerin, L. (2017) AMPK activation caused by reduced liver lactate metabolism protects against hepatic steatosis in MCT1 haploinsufficient mice. *Mol. Metab.*, **6**, 1625-1633.
35. Baltazar, F., Afonso, J., Costa, M. and Granja, S. (2020) Lactate Beyond a Waste Metabolite: Metabolic Affairs and Signaling in Malignancy. *Front. Oncol.*, **10**, 231.

36. De Saedeleer, C.J., Copetti, T., Porporato, P.E., Verrax, J., Feron, O. and Sonveaux, P. (2012) Lactate activates HIF-1 in oxidative but not in Warburg-phenotype human tumor cells. *PLoS One*, **7**, e46571.
37. Belibi, F., Zafar, I., Ravichandran, K., Segvic, A.B., Jani, A., Ljubanovic, D.G. and Edelstein, C.L. (2011) Hypoxia-inducible factor-1alpha (HIF-1alpha) and autophagy in polycystic kidney disease (PKD). *Am. J. Physiol. Renal. Physiol.*, **300**, F1235-1243.
38. Kraus, A., Peters, D.J.M., Klanke, B., Weidemann, A., Willam, C., Schley, G., Kunzelmann, K., Eckardt, K.U. and Buchholz, B. (2018) HIF-1alpha promotes cyst progression in a mouse model of autosomal dominant polycystic kidney disease. *Kidney. Int.*, **94**, 887-899.
39. Li, A., Xu, Y., Fan, S., Meng, J., Shen, X., Xiao, Q., Li, Y., Zhang, L., Zhang, X., Wu, G. *et al.* (2018) Canonical Wnt inhibitors ameliorate cystogenesis in a mouse ortholog of human ADPKD. *JCI Insight*, **3**.
40. Lee, E.J., Seo, E., Kim, J.W., Nam, S.A., Lee, J.Y., Jun, J., Oh, S., Park, M., Jho, E.H., Yoo, K.H. *et al.* (2020) TAZ/Wnt-beta-catenin/c-MYC axis regulates cystogenesis in polycystic kidney disease. *Proc. Natl Acad. Sci. U S A*, **117**, 29001-29012.
41. Idowu, J., Home, T., Patel, N., Magenheimer, B., Tran, P.V., Maser, R.L., Ward, C.J., Calvet, J.P., Wallace, D.P. and Sharma, M. (2018) Aberrant Regulation of Notch3 Signaling Pathway in Polycystic Kidney Disease. *Sci. Rep.*, **8**, 3340.
42. Formica, C. and Peters, D.J.M. (2020) Molecular pathways involved in injury-repair and ADPKD progression. *Cell Signal.*, **72**, 109648.
43. Takakura, A., Contrino, L., Zhou, X., Bonventre, J.V., Sun, Y., Humphreys, B.D. and Zhou, J. (2009) Renal injury is a third hit promoting rapid development of adult polycystic kidney disease. *Hum. Mol. Genet.*, **18**, 2523-2531.
44. Podrini, C., Rowe, I., Pagliarini, R., Costa, A.S.H., Chiaravalli, M., Di Meo, I., Kim, H., Distefano, G., Tiranti, V., Qian, F. *et al.* (2018) Dissection of metabolic reprogramming in polycystic kidney disease reveals coordinated rewiring of bioenergetic pathways. *Commun. Biol.*, **1**, 194.
45. Perrone, R.D., Abebe, K.Z., Watnick, T.J., Althouse, A.D., Hallows, K.R., Lalama, C.M., Miskulin, D.C., Seliger, S.L., Tao, C., Harris, P.C. *et al.* (2021) Primary results of the randomized trial of metformin administration in polycystic kidney disease (TAME PKD). *Kidney Int.*, **100**, 684-696.
46. Prikis, M., Mesler, E.L., Hood, V.L. and Weise, W.J. (2007) When a friend can become an enemy! Recognition and management of metformin-associated lactic acidosis. *Kidney Int.*, **72**, 1157-1160.
47. Scheen, A.J. and Paquot, N. (2013) Metformin revisited: a critical review of the benefit-risk balance in at-risk patients with type 2 diabetes. *Diabetes Metab.*, **39**, 179-190.

48. Memmott, R.M., Mercado, J.R., Maier, C.R., Kawabata, S., Fox, S.D. and Dennis, P.A. (2010) Metformin prevents tobacco carcinogen--induced lung tumorigenesis. *Cancer Prev. Res. (Phila)*, **3**, 1066-1076.
49. Subramanian, A., Kuehn, H., Gould, J., Tamayo, P. and Mesirov, J.P. (2007) GSEA-P: a desktop application for Gene Set Enrichment Analysis. *Bioinformatics*, **23**, 3251-3253.

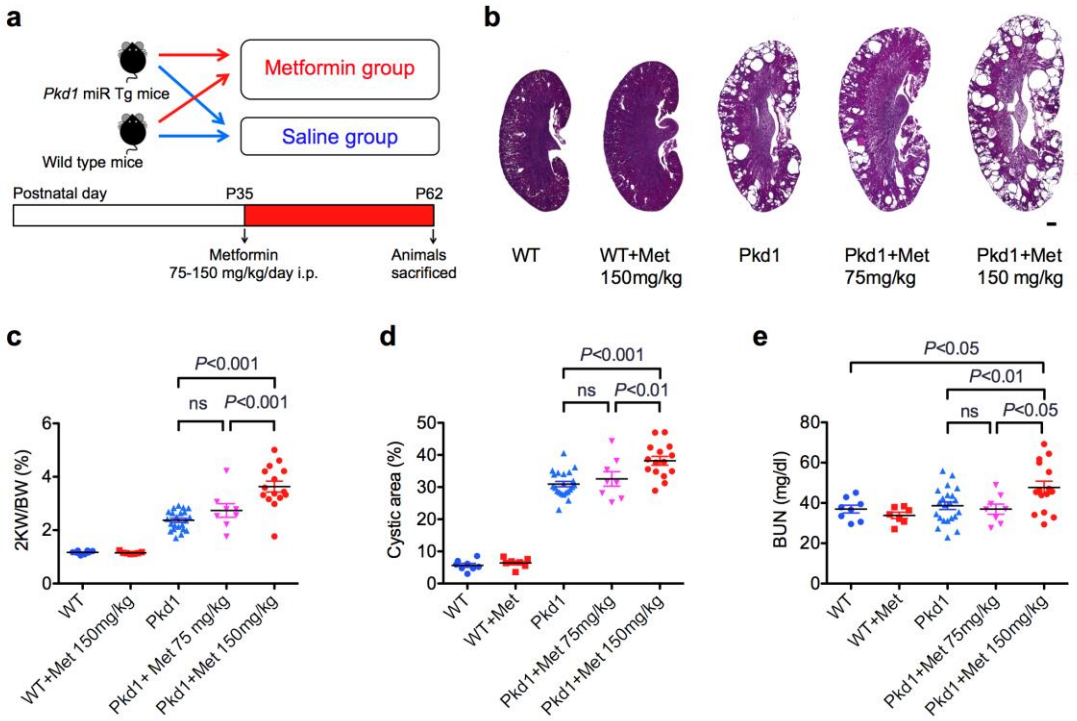

Figure 1. Metformin treatment exacerbates the cystic phenotype in *Pkd1* miR Tg mice. (a) Schematic outline of metformin administration and experimental groups. (b) Images of H & E stained kidney sections showing the enlarged cystic kidney in metformin-treated *Pkd1* miR Tg mice compared to vehicle-treated *Pkd1* mutant mice and wild-type mice. (c) Comparisons of two-kidney-weight/body-weight (2KW/BW) ratios, (d) Cystic indices, and (e) BUN levels between different experimental groups as indicated. Mice received 4 weeks of intraperitoneal injection of metformin at a dose of 75 or 150 mg/kg/day from P35. Control groups received intraperitoneal injections of vehicle (normal saline). Data are mean ± SEM (n=8, 7, 22, 8, and 15 per group, respectively). ns, not statistically significant; Pkd1, polycystic kidney disease 1; WT, wild type. Scale bar, 1 mm.

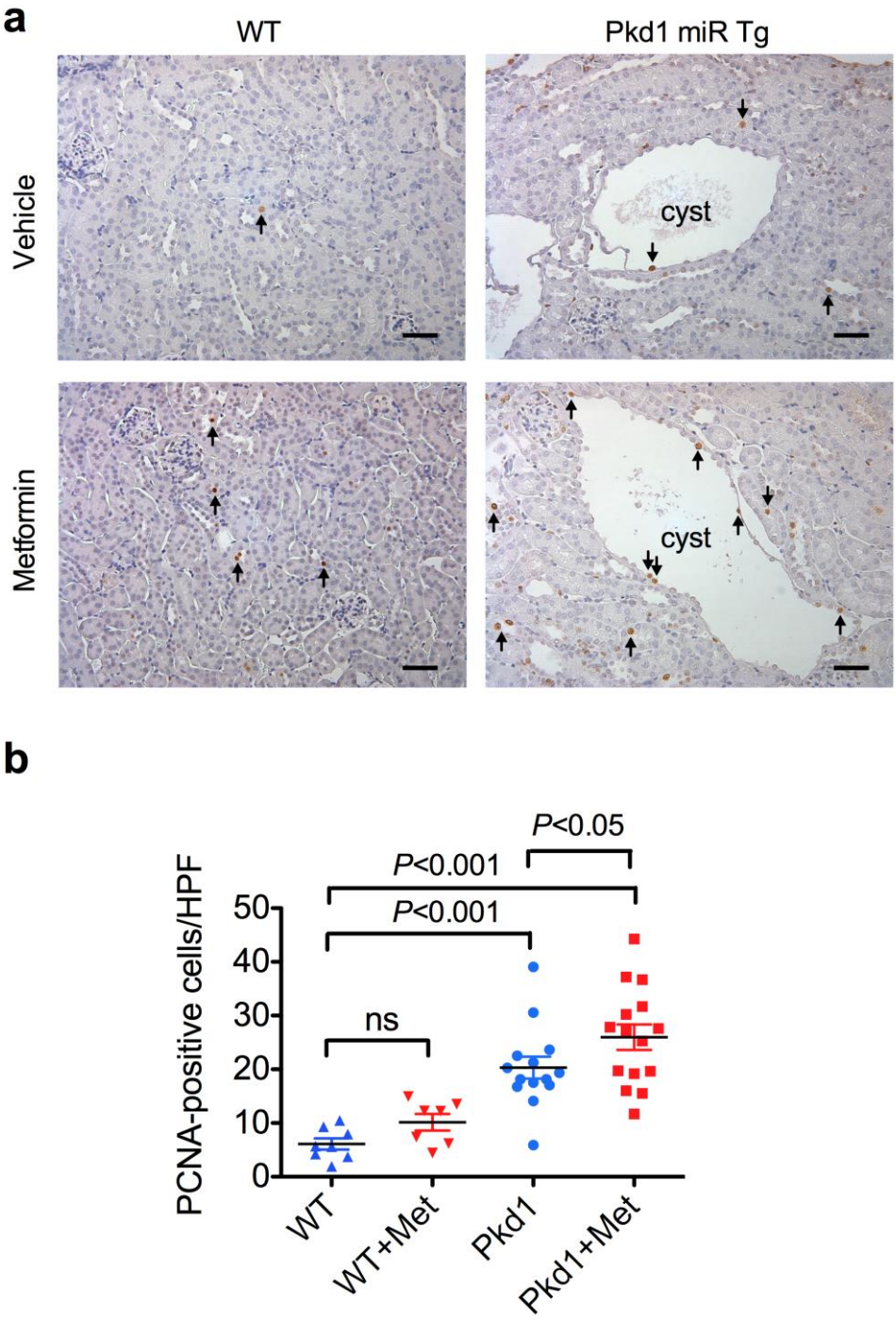

Figure 2. Metformin treatment promotes cyst growth in *Pkd1* miR Tg mice. (a) Representative images of immunohistochemistry staining for proliferating cell nuclear antigen (PCNA) showing positive nuclear staining (arrows) in cyst lining epithelial cells and non-cystic tubular cells in the kidneys. (b) Comparison of the proliferative indices in different experimental groups as indicated. Data are mean ± SEM (n=8, 7, 14, and 15 per group, respectively). Scale bar, 50 μm.

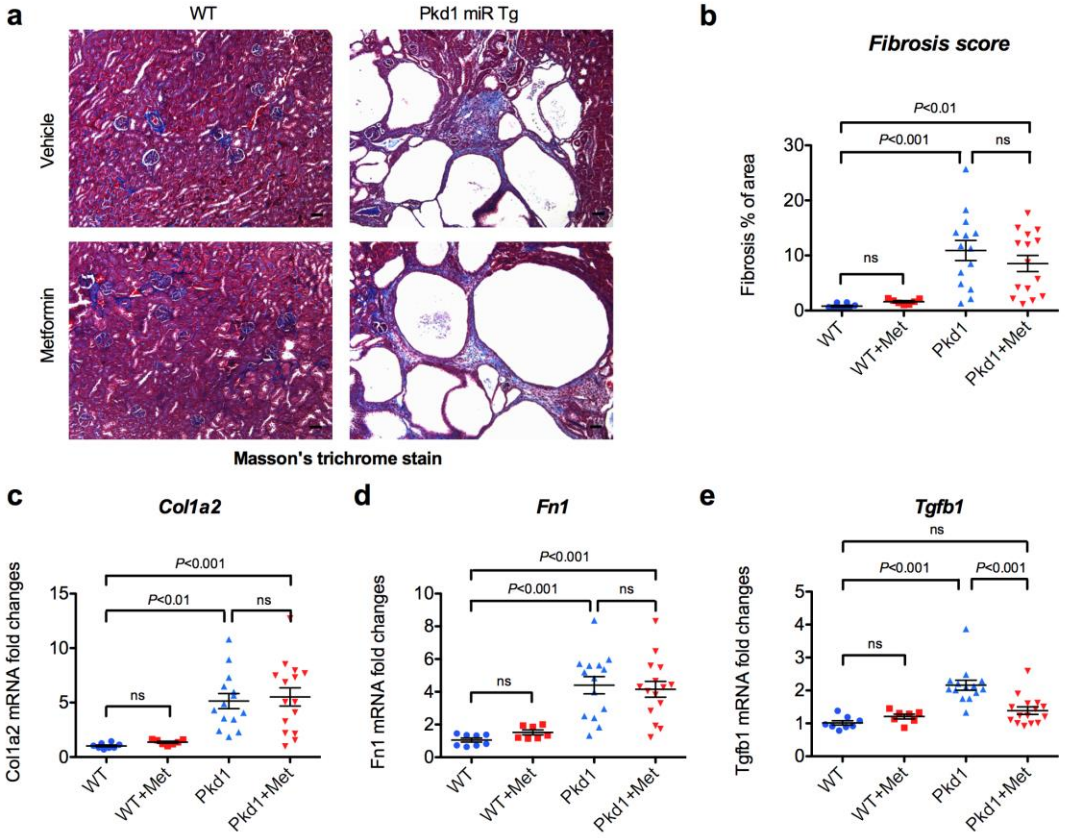

Figure 3. Effects of metformin treatment on renal fibrosis in *Pkd1*-deficient mice. (a) Masson's trichrome staining of kidney sections from wild-type and *Pkd1* miR Tg mice with or without metformin treatment (150 mg/kg/day). Scale bar, 50 μm, (b) Comparison of renal fibrosis by quantitative histological analysis of the kidney sections. Renal mRNA expression of (c) *Col1a2,* (d) *Fn1,* and (e) *Tgfb1* by qRT-PCR analysis are shown. The internal control gene used for normalization was *tbp*. Data are mean ± SEM (n=8,7.14, and 15 per group, respectively). Scale bar, 50 μm.

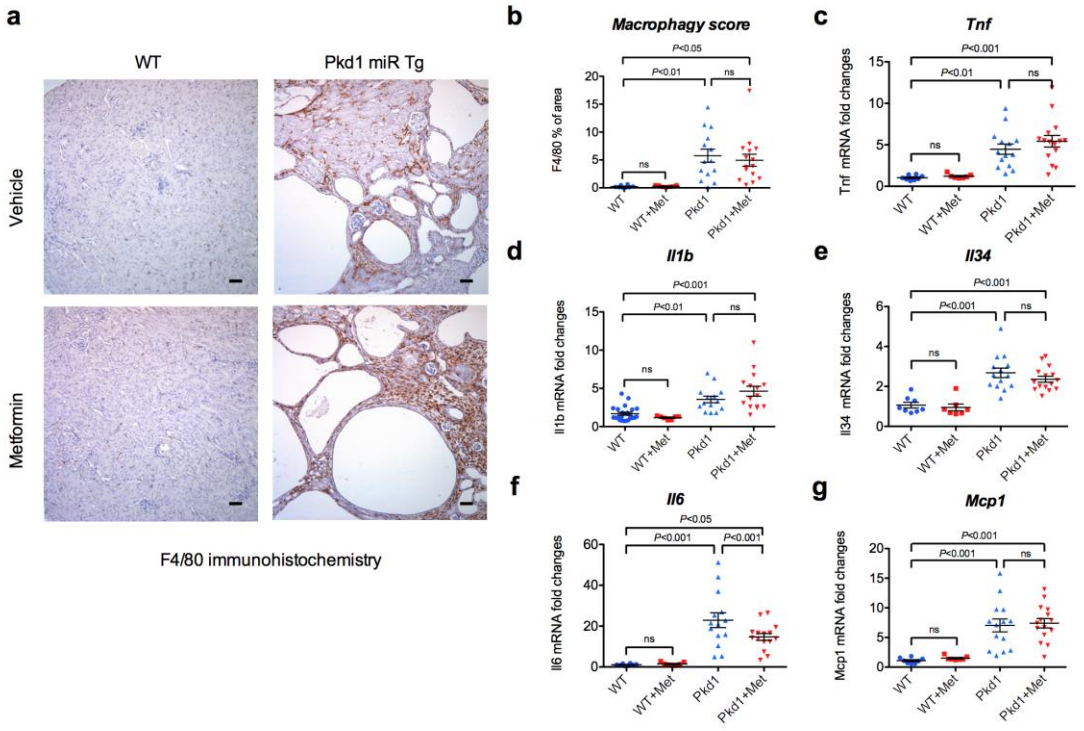

Figure 4. Effects of chronic metformin treatment on renal inflammation in *Pkd1*-deficient mice. (a) F4/80 immunostaining for kidney sections from wild-type and *Pkd1* miR Tg mice and the effects of metformin treatment (150 mg/kg/day). Scale bar, 50 µm. (b) Comparison of the percentage areas of F4/80-positive macrophages by quantitative histological analysis, Relative renal mRNA expression of (c)*Tnf*, (d) *Il1b*, (e) *Il6*, (f) *Mcp1*, and (g) *Il34* by qRT-PCR analysis are shown. The internal control gene used for normalization was *tbp*. Data are mean ± SEM (n=8,7,14,15 per group, respectively). Scale bar, 50 µm.

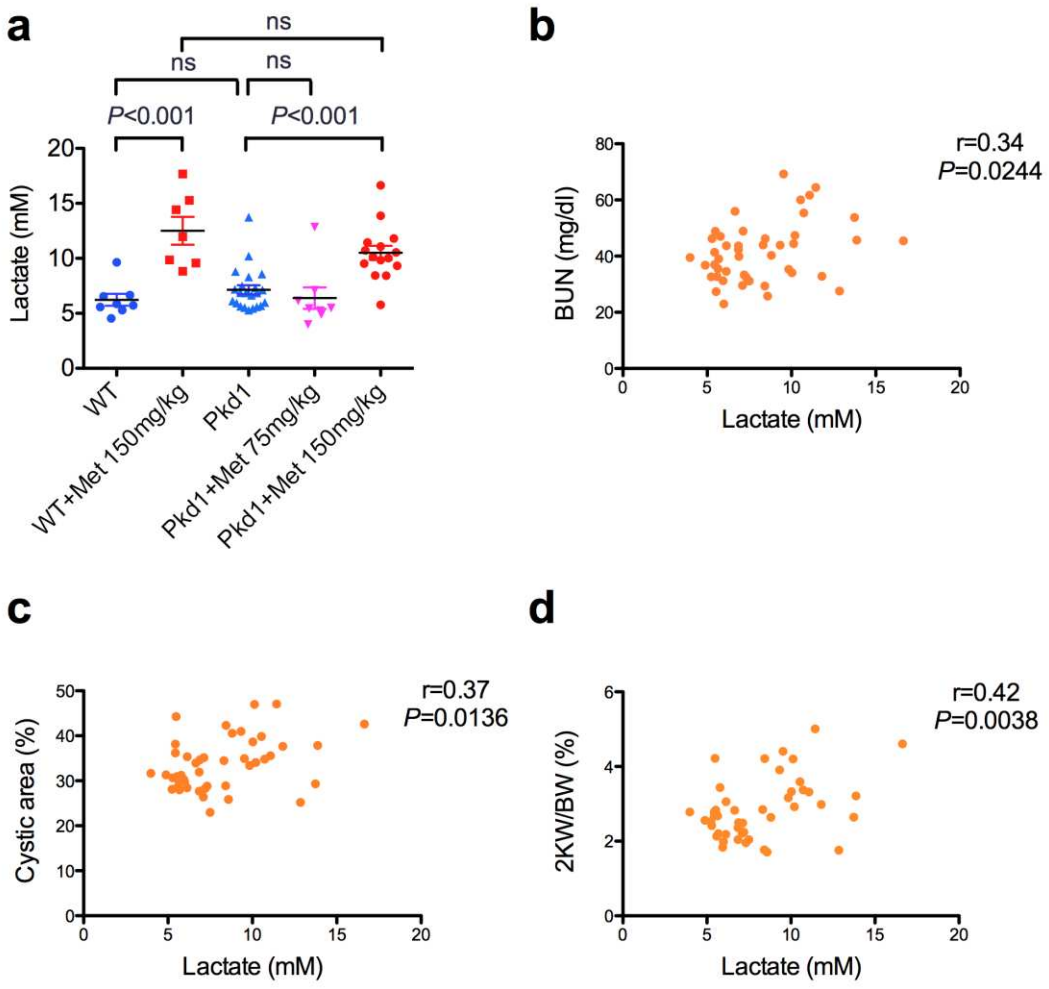

Figure 5. Effect of metformin treatment on plasma lactate levels in wild-type and *Pkd1* miR Tg mice. (a) Note chronic metformin treatment (150 mg/kg/day intraperitoneally for 28 days) resulted in a significant elevation of plasma lactate levels. Data are mean ± SEM (n=8, 7, 22, 8, and 15 per group, respectively). Plasma lactate levels were significantly correlated with (b) BUN levels (r=0.34, $P<0.05$), (c) Cystic indices (r=0.37, $P<0.05$), and (d) Two-kidney-weight/body-weight (2KW/BW) ratios (r=0.42, $P<0.01$) in *Pkd1* miR Tg mice.

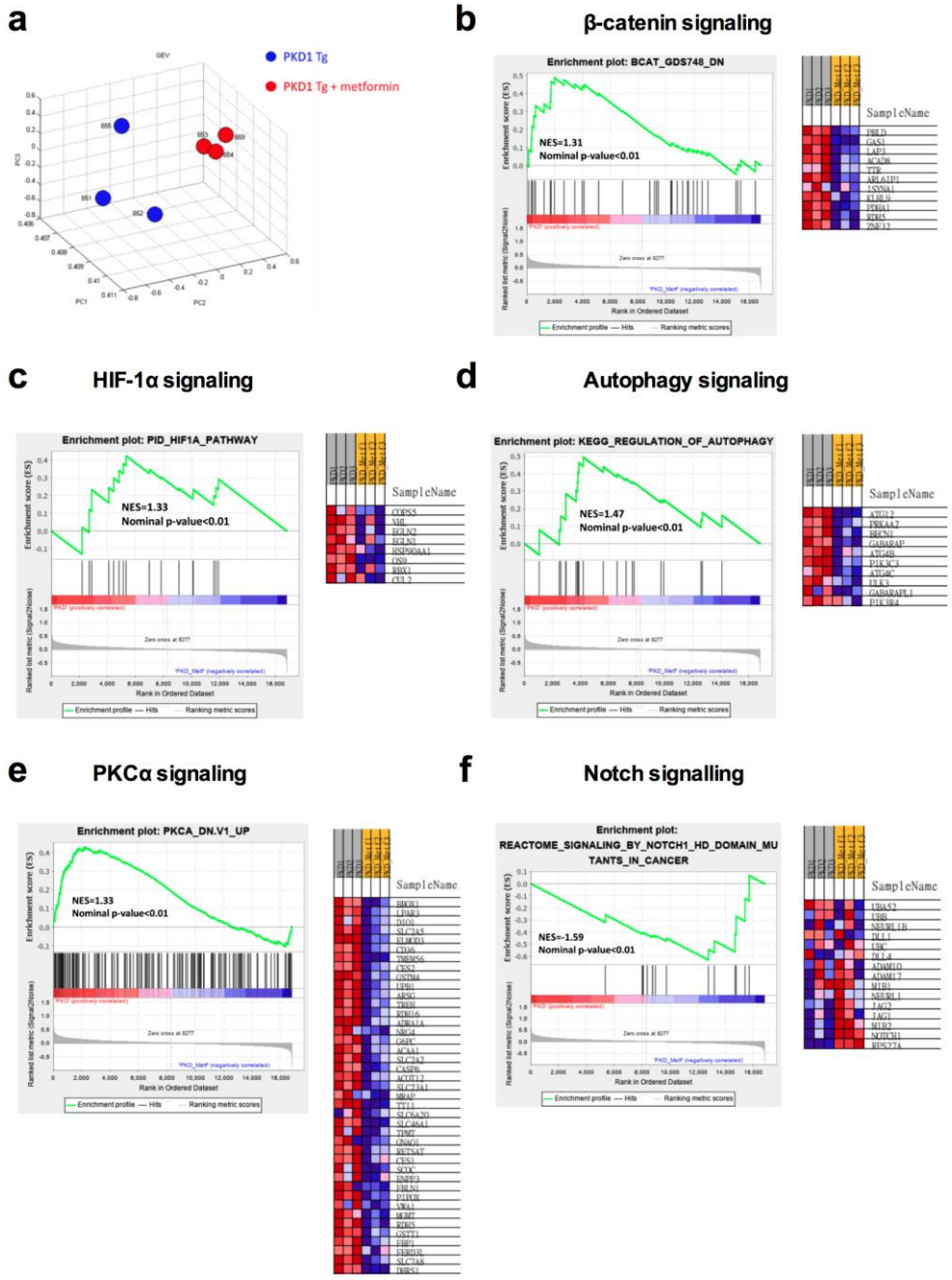

Figure 6. Correlation of pro-proliferative pathways with microarray differential gene expression data using Gene Set Enrichment Analysis (GSEA). (a) Three dimensional scatter plot from Principal Component Analysis of the microarray data showing the differential gene expression in the kidneys from *Pkd1* mutant+vehicle vs *Pkd1*+metformin (150 mg/kg/day; n=3 per group). GSEA plots of (b) β-catenin (dominant-negative), (c) HIF-1α (negative regulatory), (d) autophagy, (e) PKCα (dominant-negative), and (f) Notch networks. NES: normalized enrichment score. Heatmap display of the differentially expressed genes (>2 fold) in each group is shown along with the GSEA plot.

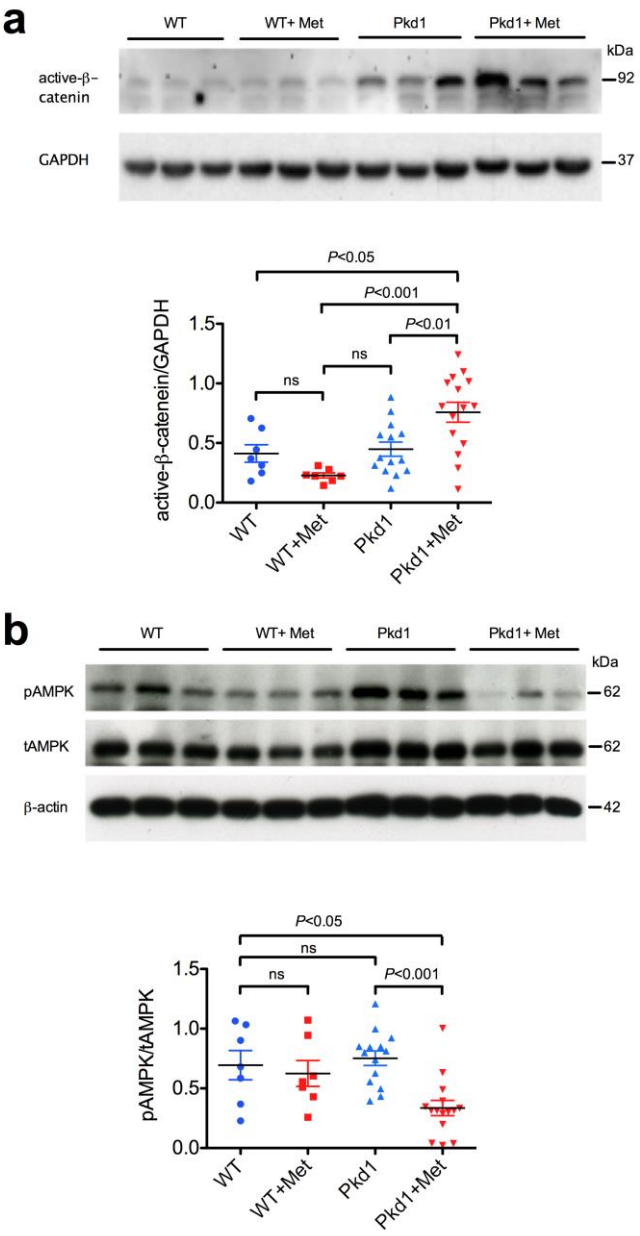

Figure 7. Metformin enhances the expression of active β-catenin and suppresses the phosphorylation of AMPK in *Pkd1* miR Tg mice. Kidney lysates from *Pkd1* miR Tg mice and wild-type mice with or without metformin treatment (150 mg/kg/day i.p. for 28 days) were analyzed by Western blotting. (a) Representative immunoblots of active β-catenin and GAPDH. The densitometry results of active β-catenin were normalized to GAPDH (b) Representative immunoblots of phosphorylated AMPK, total AMPK, and β-actin. The densitometric results of p-AMPK were normalized to t-AMPK. Data are mean ± SEM (n=7-15 per group).

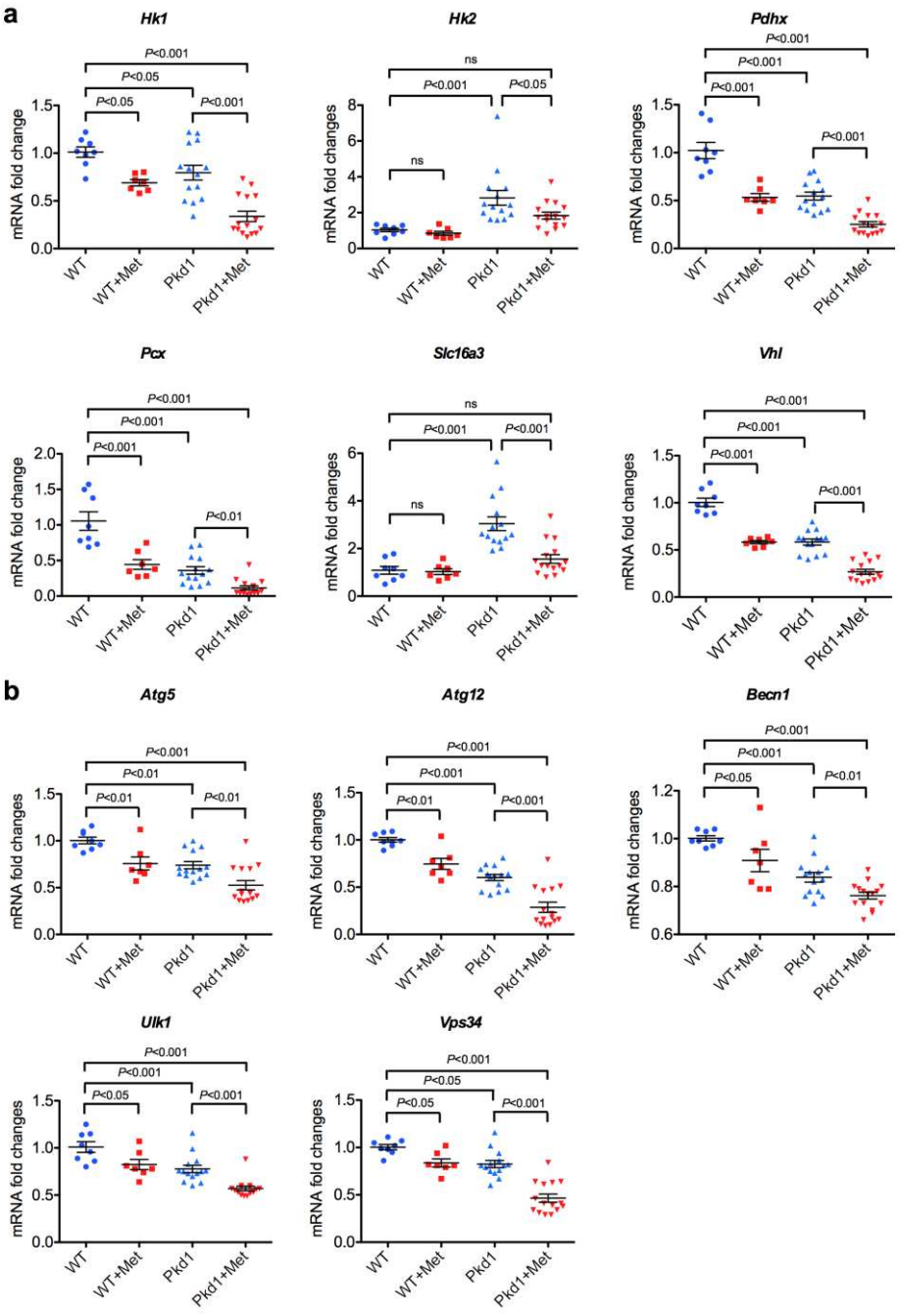

Figure 8. Effects of metformin treatment on the expression of genes related to glycolysis and autophagy. qRT-PCR analysis of the kidneys showed the effects of metformin treatment (150 mg/kg/day i.p. for 4 weeks) on the renal mRNA expression of (a) Glycolysis genes: *Hk1, Hk2, Pdhx, Pcx, Slc16a3,* and *Vhl,* and (b) Autophagy genes: *Atg5, Atg12, Becn1, Ulk1,* and *Vps34.* These genes were significantly downregulated in *Pkd1* miR Tg mice treated with metformin compared to those treated with saline. Data are mean ± SEM (n=7-15 per group).

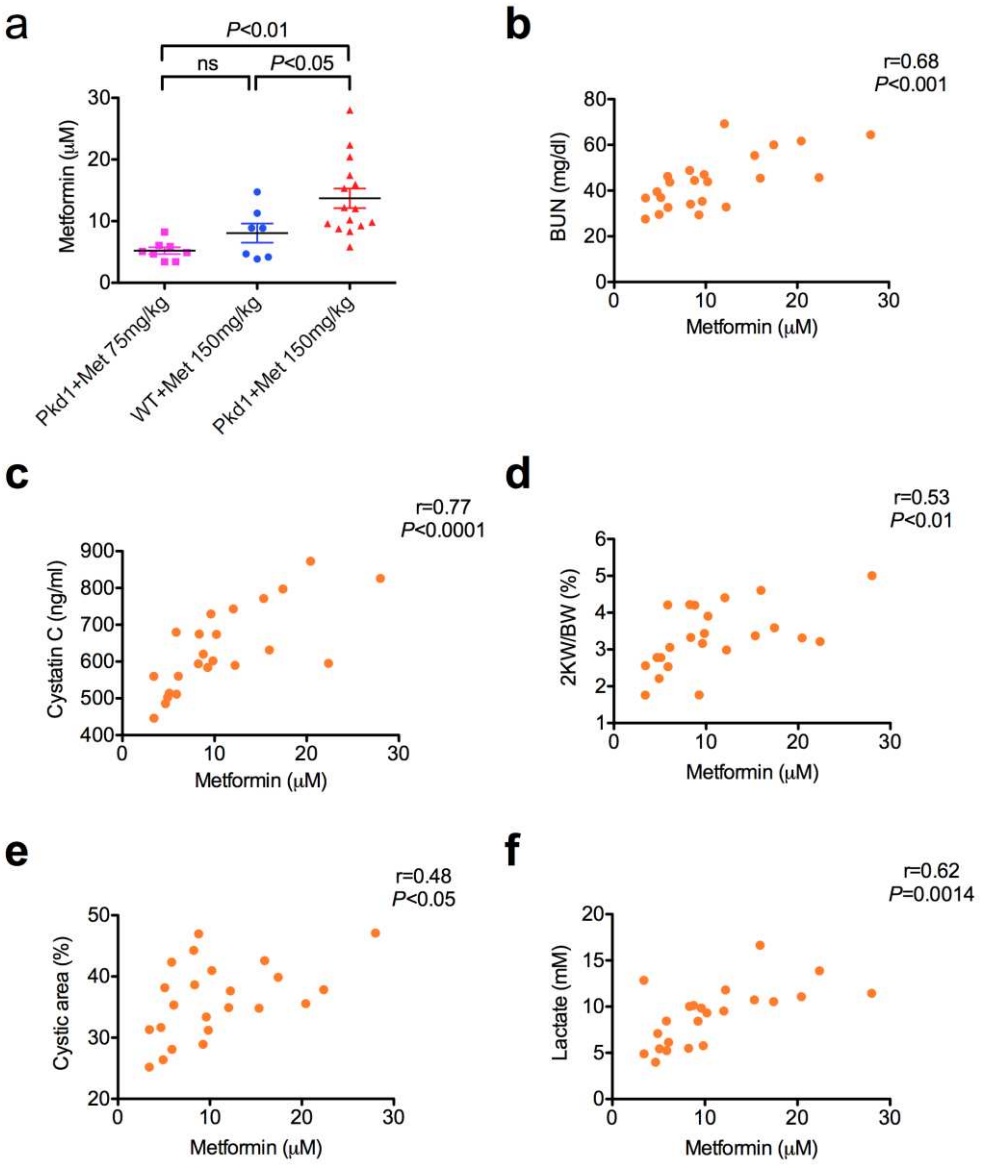

Figure 9. Correlations between blood metformin concentrations and kidney function. *Pkd1* miR Tg mice and wild type mice were treated with metformin (75 to 150 mg/kg/day i.p.) from P35 to P62. (a) Plasma metformin concentrations were determined by liquid chromatography-mass spectrometry (LC-MS). Data are mean ± SEM. Metformin concentrations were significantly correlated with (b) BUN levels (r=0.68, P<0.001), (c) Cystatin C levels (r=0.77, P<0.0001), (d) Two-kidney-weight/body-weight (2KW/BW) ratios (r=0.53, P<0.01), (e) Cystic indices (r=0.48, P<0.05), and (f) Plasma lactate levels (r=0.62, P<0.01) by the Pearson correlation test. (Wild-type: n=7 for 150 mg/kg, *Pkd1*: n=8 for 75 mg/kg, n=15 for 150 mg/kg)

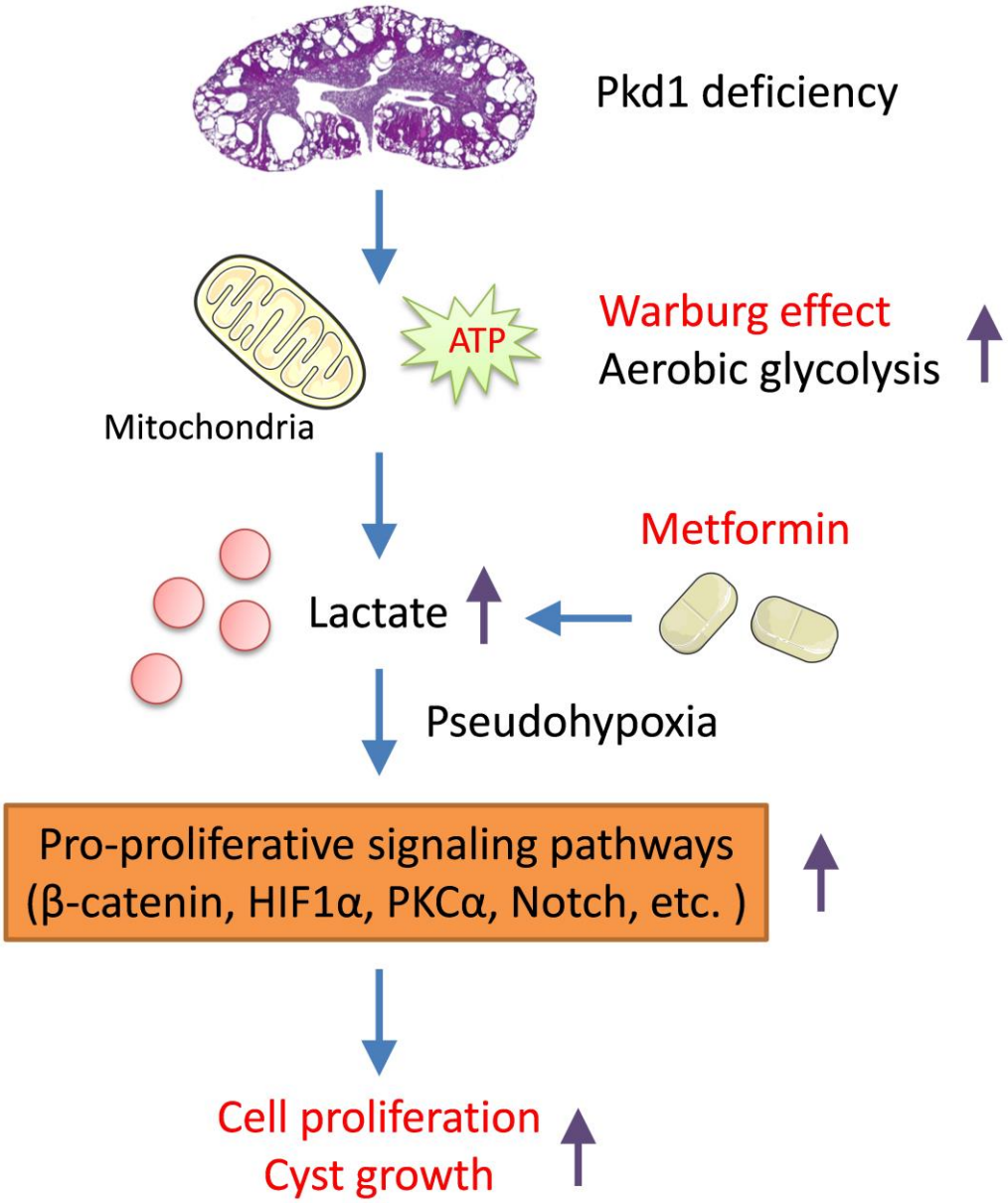

Figure 10. Metformin exacerbates cyst growth in later-stage ADPKD. A working model showing metformin could induce lactate accumulation, activate pro-proliferative pathways, and promote cyst growth in later-stage of ADPKD. The graphical illustration was prepared using images from Servier Medical Art by Les Laboratoires Servier (https://smart.servier.com/).

Supplementary Materials

1. **Supplementary Figure S1.** No significant gender effects of metformin treatment in *Pkd1* miR Tg mice.
2. **Supplementary Figure S2.** Measurement of transgenic copy number of *Pkd1* miR Tg mice.
3. **Supplementary Figure S3.** Effects of metformin treatment on cyst progression and renal function in *Pkd1* $^{RC/RC}$ mice
4. **Supplementary Figure S4.** A heat map presentation of the top 100 differentiated expressed genes in vehicle-treated *Pkd1* miR TG mice (control) compared to metformin-treated *Pkd1* miR TG mice (treatment) using microarray analyses.
5. **Supplementary Figure S5.** Effects of metformin on mTOR phosphorylation in *Pkd1* miR Tg mice.
6. **Supplementary Figure S6.** Effects of metformin on ERK phosphorylation in *Pkd1* miR Tg mice.
7. **Supplementary Table S1.** Taqman probe ID and primer sequences used for quantitative real-time PCR.
8. **Supplementary Table S2.** Effects of metformin treatment on the biochemical parameters in *Pkd1* miR Tg mice

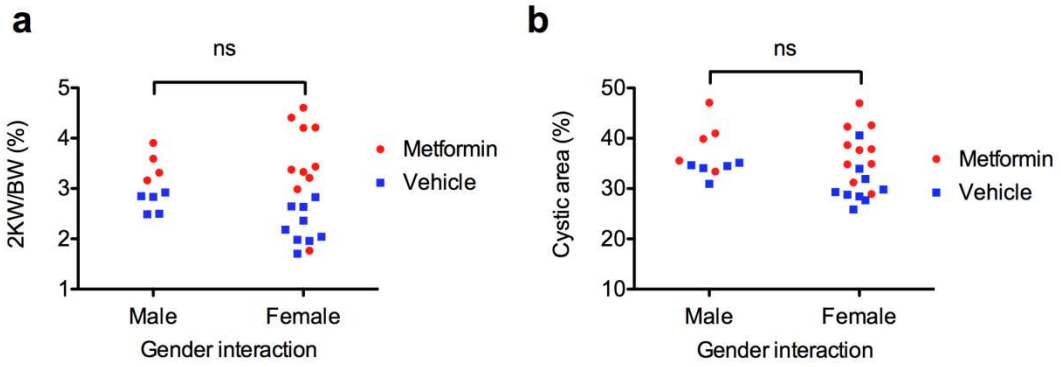

Supplementary Figure S1. No significant gender effects of metformin treatment. (a) Two-kidney-weight/body-weight (2KW/BW) ratios and (b) Cyst indices in *Pkd1* miR Tg mice treated with metformin (150mg/kg/day i.p.) or vehicle controls from P35 to P62. A two-way ANOVA found no significant gender effect or interaction between metformin and gender factors ($P>0.05$). A significant metformin effect was found for 2KW/BW ratios ($P<0.0001$) and cyst indices ($P<0.01$). Male, n=10; female n=19.

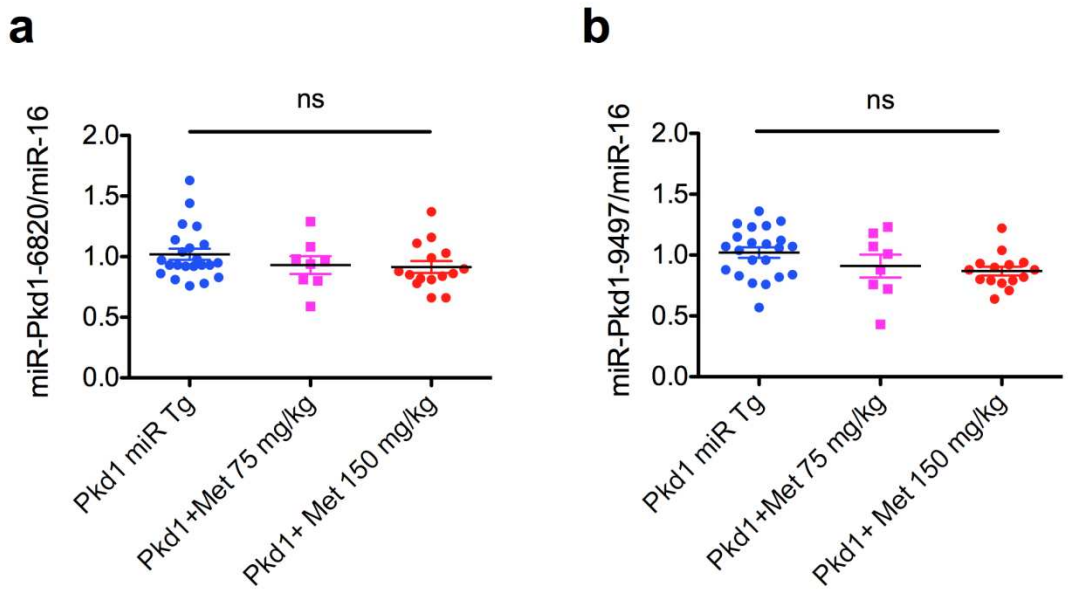

Supplementary Figure S2. Measurement of transgenic copy number of Pkd1 miR Tg mice. miRNA-specific qRT-PCR revealed no significant differences in the expression of transgenic *Pkd1*-miRNA 6820 and 9497 between the different treatment groups (n=22, 8, and 15 per group, respectively). The internal control used for normalization was miR-16.

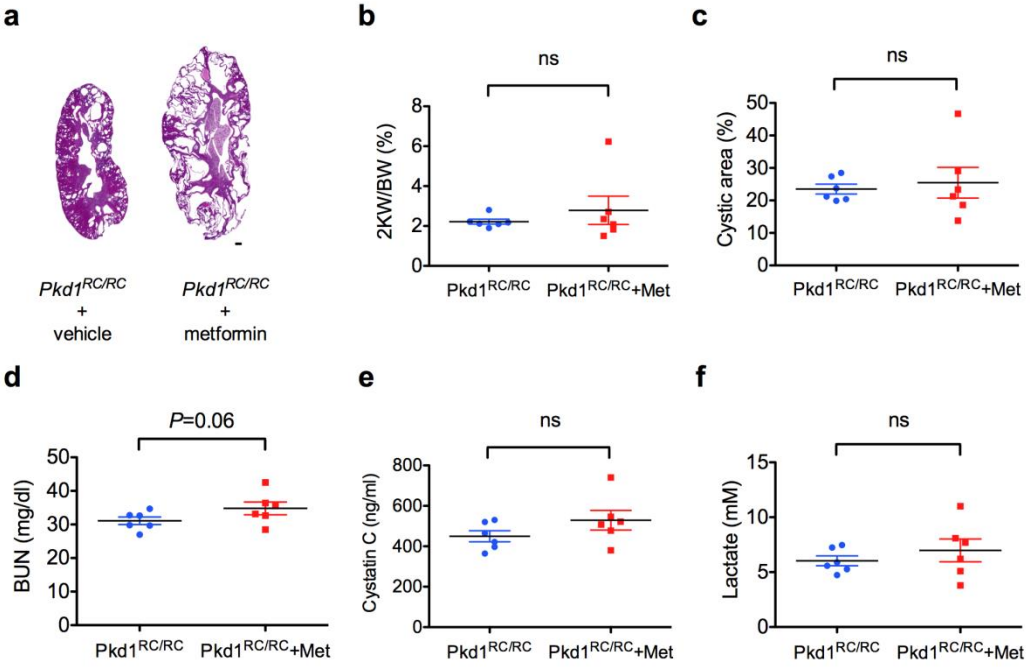

Supplementary Figure S3. Effects of metformin on cyst progression and renal function in *Pkd1*$^{RC/RC}$ mice. (a) Representative H & E stained kidney sections from the most severely affected control and metformin-treated *Pkd1*$^{RC/RC}$ mice. Comparisons of (b) two-kidney-weight/body-weight (2KW/BW) ratios, (c) cyst indices, (d) BUN, (e) cystatin C, and (f) plasma lactate levels between control and treatment groups. *Pkd1* $^{RC/RC}$ mice on the C57BL/6 background (n=6 males per group) were randomized to receive either i.p. injections of metformin (150 mg/kg/day) or saline vehicle from P35 to P64. Data are mean ± SEM. One-sided Student`s t-test was used to compare the means of two groups. Scale bar, 1 mm.

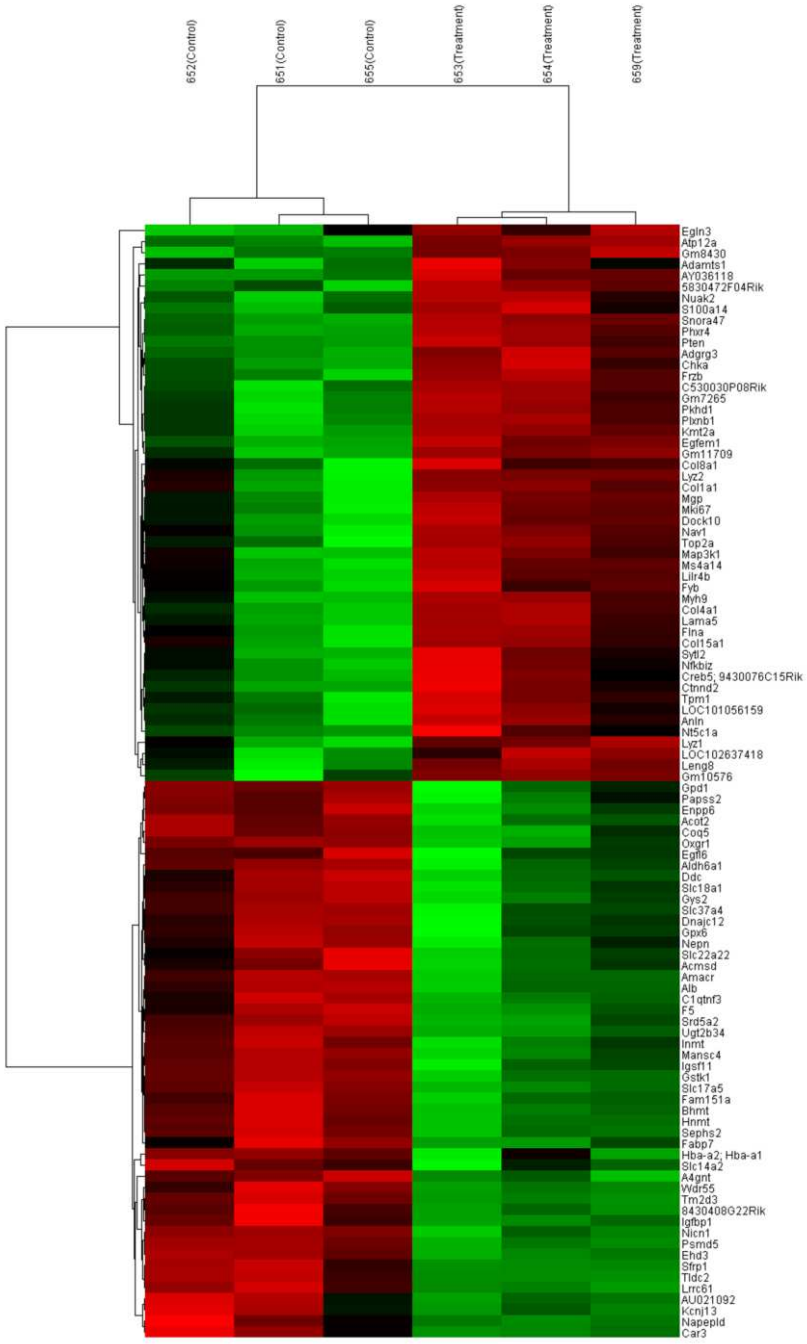

Supplementary Figure S4. A heat map presentation of the top 100 differentiated expressed genes in vehicle-treated *Pkd1* miR TG mice (control) compared to metformin-treated *Pkd1* miR TG mice (treatment) using microarray analyses. The mice were treated with i.p. metformin (150 mg/kg) or saline for 4 weeks. The threshold was set at the fold change of relative expression of greater than two-fold and $p < 0.05$. Red, upregulation; green, downregulation.

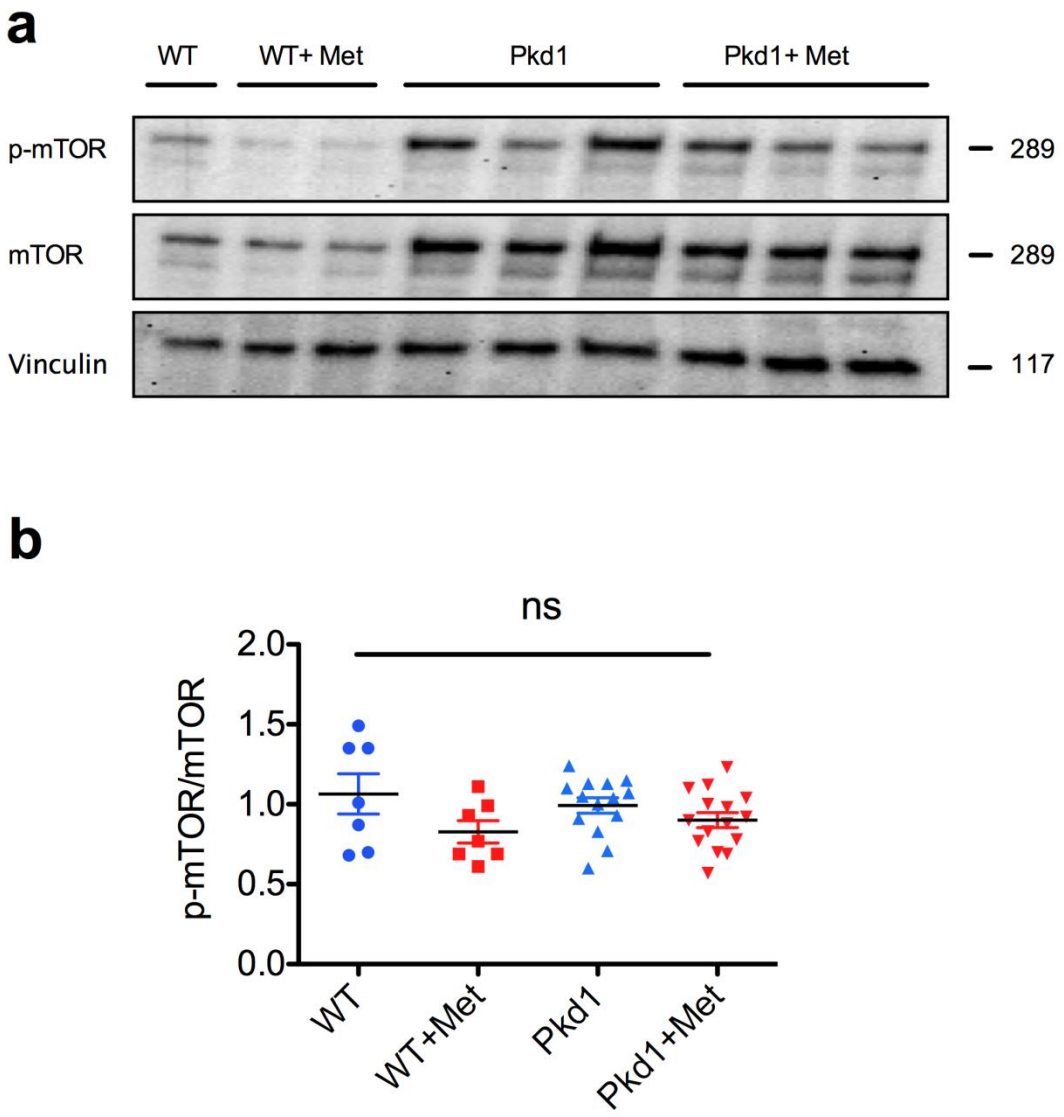

Supplementary Figure S5. Effects of metformin on the mTOR phosphorylation in *Pkd1* miR Tg mice. Kidney lysates from *Pkd1* miR Tg and wild-type mice treated with metformin (150 mg/kg/day i.p.) or saline vehicle controls were analyzed by Western blotting using anti-phospho-mTOR (Ser2448) and anti-mTOR antibodies (Cell Signaling). (a) Representative immunoblots of p-mTOR, mTOR, and vinculin (loading control). (b) The densitometric results of p-mTOR were normalized to mTOR (n= 7-15 per group).

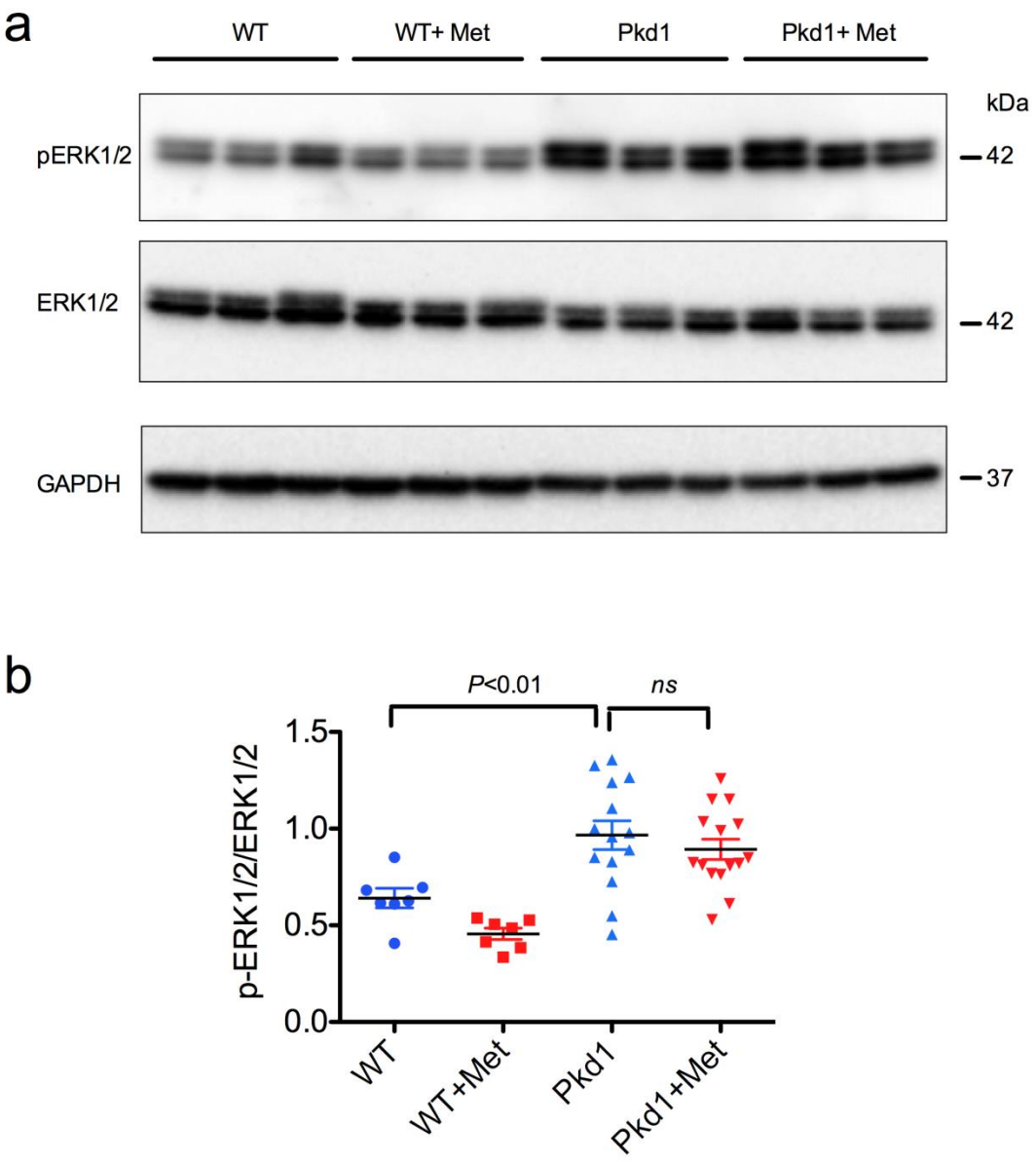

Supplementary Figure S6. Effects of metformin on the ERK phosphorylation in *Pkd1* miR Tg mice. Kidney lysates from *Pkd1* miR Tg and wild-type mice treated with metformin (150 mg/kg/day i.p.) or saline vehicle controls were analyzed by Western blotting using anti-phospho-ERK1/2 and anti-ERK1/2 antibodies (Cell Signaling). (a) Representative immunoblots of p-ERK1/2, ERK1/2, and GAPDH (loading control). (b) The densitometric results of p-ERK1/2 were normalized to ERK1/2 (n= 7-15 per group).

Supplementary Table S1. Taqman probe ID and primer sequences used for quantitative real-time PCR

Gene	*Taqman probe or primer sequences (5' to 3')*
Atg5	Mm01187303_m1
Atg12	Mm00503201_m1
Becn1	Mm01265461_m1
Col1a2	F: AAGGGGTCTTCCTGGTGAAT; R: GGGGTACCACGTTCTCCTC
Fn1	F: TGTGACCAGCAACACGGTG; R: ACAACAGGAGAGTAGGGCGC
Hk1	Mm00439344_m1
Hk2	Mm00443385_m1
Il1b	Mm00434228_m1
Il34	Mm01243248_m1
Il6	Mm01210733_m1
Mcp1	Mm00441242_m1
Pcx	Mm00500992_m1
Pdhx	Mm00558275_m1
Slc16a3	Mm00446102_m1
Tbp	Mm00446973_m1
Tgfb1	F: TGCGTCTGCTGAGGCTCAA; R: TTGCTGAGGTATCGCCAGGA
Tnf	Mm99999068_m1
Ulk1	Mm00437238_m1
Vhl	Mm00494137_ml
Vps34	Mm00619489_m1

Supplementary Table S2. Effects of metformin treatment on the biochemical parameters in *Pkd1* miR Tg mice

	WT+S (n=8)	**WT+Met (n=7)**	**Pkd1+S (n=22)**	**Pkd1+Met 75 mg/kg (n=8)**	**Pkd1+Met 150 mg/kg (n=15)**
Gender (M/F)	3/5	3/4	8/14	3/5	5/10
BUN (mg/dl)	37.0 ± 2.0	33.9 ± 1.6	38.6 ± 2.5	36.9 ± 2.5	47.7 ± 3.1$^{*, \#\#}$
Plasma cystatin C (ng/ml)	527.8 ± 20.5	589.7 ± 30.5	599.6 ± 21.1	521.7± 16.8	692.7 ± 24.0$^{***, \#}$
Blood glucose, day 48 (mg/dl)	161 ± 11	177 ± 11	140 ± 6	130 ± 10	141± 7
Blood glucose, day 61 (mg/dl)	177 ± 5	175± 5	174± 12	139 ± 7	166± 12

Data are mean ± SEM. Met, metformin; Pkd, polycystic kidney disease; S, saline; WT, wild-type.

$^{*}P < 0.05$, $^{**}P < 0.01$, and $^{***}P < 0.001$ versus wild-type mice + saline.

$^{\#}P < 0.05$, $^{\#\#}P < 0.01$ versus *Pkd1* miR Tg mice + saline.